ABSTRACT

AILSWORTH JR, JAMES WILLIAM. Development of Neurofeedback Therapies for Hand Rehabilitation in Stroke. (Under the direction of Dr. Kamper).

In this work, a number of novel neurofeedback interventions targeting neuromuscular impairment are described. Populations who ultimately may benefit from these interventions include stroke survivors and individuals with Parkinson's Disease. We first describe a device that re-trains aberrant cortical and muscular activation patterns and enables movement practice with a robotic hand exoskeleton. Next, we describe a novel approach to treating impaired flexor muscle relaxation by using brain-computer interface (BCI) training and motor imagery preceding grasp release. Finally, we use corticomuscular coherence (CMC) to investigate potential neural mechanisms for improved hand function following BCI training of muscle relaxation.

Development of Neurofeedback Therapies for Hand Rehabilitation in Stroke

by
James William Ailsworth JR

A dissertation submitted to the Graduate Faculty of
North Carolina State University
in partial fulfillment of the
requirements for the degree of
Doctor of Philosophy

Biomedical Engineering

Raleigh, North Carolina
2023

APPROVED BY:

_____	_____
Dr. Derek Kamper Committee Chair	Dr. Xiaogang Hu
_____	_____
Dr. Chang Nam	Dr. Jessica Cassidy
_____	
Dr. Helen Huang	

BIOGRAPHY

James Ailsworth JR earned his Bachelor's degree in biomedical engineering from Virginia Commonwealth University in 2013. He then earned a Master's degree in mechanical engineering from Virginia Tech in 2016 developing novel brain-computer interface algorithms for his thesis research. James then joined Derek Kamper's laboratory at NC State in 2017 and continued his work in brain-computer interface technology for the application of hand rehabilitation in stroke survivors.

TABLE OF CONTENTS

LIST OF TABLES

LIST OF FIGURES

CHAPTER 1: INTRODUCTION

1.1 Significance

A stroke occurs when there is an interruption of blood flow and oxygen to the brain resulting in the death of brain cells within minutes. About 795,000 people experience a new (610,000) or recurrent (185,000) stroke in the U.S. each year. While roughly 137,000 people will die from their stroke [1,2], recognition of the signs of stroke and improvements in acute care have greatly reduced the one-year mortality rates [1]. Thus, 9.4 million stroke survivors live in the U.S. [1] Despite rehabilitation efforts, however, a majority of stroke survivors will experience chronic impairment [1], typically involving both the upper and lower extremity on one side of the body. Indeed, stroke is the leading cause of long-term serious disability [1] with around 22-40% of stroke survivors having chronic moderate to severe disability [3]. As stroke can occur at relatively young age (in one study, 38% of people hospitalized for a stroke were under 65 years of age [4]), individuals may live with this disability for many years. In total, stroke-related costs in the U.S., including cost of health care services, medicines to treat stroke, and missed days of work, accounted for nearly $56.5 billion between 2018 and 2019. [1].

Impairment is especially likely to occur in the hand [5-6]. Due to the importance of the hand to everyday activities, hand impairment can substantially impact employment, self-care, and quality of life. Use of our hands can hardly be overstated as they are our primary means of interacting with the external world.

1.2 Impaired Object Manipulation after Stroke

Although deceptively simple to the unimpaired, object manipulation actually involves the coordination of a complex sequence of movements. These include hand opening and shaping to grasp an object, grip force generation, object transport, and object release. These may all be

impacted by the stroke. Stroke survivors experience poor hand opening and grasp shaping [7], improperly directed grasping forces and weakness [8], abnormal synergies during object transport [9], and delays in muscle deactivation resulting in difficulty completing activities of daily living [10].

1.3 Neural Basis for Hand Impairment

Complex movements such as object manipulation involve four basic phases that overlap in time: planning, initiation, execution, and termination. Movement planning and initiation take place in the cerebral cortex and can be studied using electroencephalography (EEG). Likewise, movement execution and termination take place in the spinal cord and muscles and can be studied using electromyography (EMG). Using these two technologies, it has been found that aberrant neural activation patterns are primarily responsible for sensorimotor deficits after stroke.

During the movement planning and initiation phase, stroke survivors display a weakened event-related desynchronization (ERD) of the sensorimotor rhythm (SMR) over the damaged hemisphere [11-13]. During movement execution, stroke survivors display patterns of spasticity [14], excessive co-activation of the finger flexors [15], and limited voluntary activation of finger extensors [16]. During movement termination, stroke survivors experience sustained involuntary activation of finger flexor muscles that may lead to difficulty releasing objects [17].

1.4 Cortical Involvement in Grasp Termination

Using functional imaging and electrophysiological studies, it was found that muscle relaxation is normally preceded by activation in the primary motor cortex (M1) and supplementary motor area (SMA) [18-23]. This has been suggested to reflect either the activation of corticospinal projection neurons onto inhibitory interneurons in the spinal cord and/or intrinsic inhibitory interneurons in the motor cortex [24]. A number of transcranial magnetic stimulation

(TMS) [25-29] and H-reflex [30-31] studies have been performed to elucidate the precise mechanism by which increased cortical activation leads to muscle relaxation and have found evidence for both mechanisms.

Impaired control of intracortical inhibition has been postulated to play a role in prolonged activation of flexor muscles in stroke [32-33] and in Parkinson's Disease (PD) [34-35]. Direct evidence of this for PD comes from an electroencephalography (EEG) study which found that event-related desynchronization (ERD) was delayed preceding muscle relaxation performed with the more affected hand [24]. Furthermore, it was shown that healthy elderly individuals who performed muscle relaxation at the same level as healthy young individuals did so by producing an earlier and more widespread ERD [36]. Therefore, training of ERD, such as through a brain-computer interface (BCI), could potentially benefit grasp relaxation.

1.4 Corticomuscular Coherence

Corticomuscular coherence (CMC) reflects the effective transmission of cortical oscillatory signals which travel through the corticospinal tract, synapse on spinal alpha motor neurons, and generate trains of motor unit action potentials to activate muscles. Thus, the amount of significant CMC is thought to measure the strength of supraspinal contributions to the output generated by spinal motor neurons [37]. There are several caveats to this simplified view. The shape of the motor unit action potentials varies based on the sensor location on a given muscle [37], fatigue [38], and subcutaneous tissue [39], potentially altering CMC without a change in corticospinal input. Additionally, common inputs to the spinal motor neurons, for example, from afferents of muscle spindles can reduce the CMC through a decorrelation effect without changes in corticospinal drive [40]. Despite these limitations, CMC has been found to be an effective tool for studying motor control in a wide range of muscles, populations, and tasks.

1.5 Dissertation Overview

In this dissertation, I describe our work in providing neurofeedback during the different phases of grasp-and-release. Toward this end, we developed a platform for training both EEG and EMG. We also developed a novel application of BCI: the training of grip muscle relaxation using mental imagery and BCI feedback. Finally, we will present a study using CMC to investigate potential neurological mechanisms for performance improvements following BCI training.

In Chapter 2, we will first describe the design and development of a platform that allows for training of neural activation patterns. Generation of proper neural activation drives a hand exoskeleton to enable movement practice. We will present a validation study of the device performed with neurotypical adults.

Chapter 3 describes BCI training of grasp release planning during constant-force isometric grip force control. We will present a study in neurotypical adults that tested the feasibility of this BCI application. We will then explore the spatial and spectral characteristics involved in BCI control. Finally, we will demonstrate that this novel BCI training application can lead to functional improvement.

In Chapter 4, we further explore the neurophysiological mechanisms that produced functional improvement in Chapter 3. We utilize the tool of CMC to investigate functional connectivity between the motor cortex and the muscles controlling grasp. We compare two different force control tasks (static force production and dynamic force visuomotor tracking) that were performed at baseline. We then investigate the CMC involved in the dynamic task before

and after BCI training. Finally, we analyzed the CMC during BCI control to assess if it could have had any direct impact on corticomuscular connectivity.

In Chapter 5, we will present a broad outlook on the rehabilitation potential of non-invasive neural training in light of our findings. We will summarize the lessons that we learned in our studies of neurotypical adults. Finally, we will discuss potential refinements of the technology as we transition into future studies involving stroke survivors.

CHAPTER 2: DEVELOPMENT AND VALIDATION OF AN EEG/EMG-CONTROLLED HAND EXOSKELETON FOR NEUROMUSCULAR THERAPY

***Abstract*— Hand impairment following stroke is a common outcome that currently lacks effective treatments. The primary driver of hand impairment is improper neural activation of the muscles. We describe the development of a platform for direct training of neural activation patterns using electroencephalographic (EEG) and electromyographic (EMG) feedback. The platform allows these signals to drive a hand exoskeleton in order to couple proper efferent activation to the corresponding afferent feedback. Five neurotypical subjects participated in a single-session pilot study to evaluate system performance. We found that all five participants were able to operate the system and demonstrated improved neural control over the course of training.**

2.1 Introduction

Of the 9.4 million stroke survivors currently living in the U.S. [1], around 65% will have persistent chronic hand impairment [5-6]. Due to the functional importance of the hand, this impairment can substantially impact activities of daily living and quality of life.

The underlying impairment mechanisms of stroke are believed to be predominantly neurological in origin, with changes observed at cortical and spinal levels. Electroencephalography (EEG) has revealed that stroke survivors have event-related (de)synchronization (ERD/ERS) hemispheric asymmetry during paretic hand movement and motor imagery [11-13]. Additionally, electromyography (EMG) has shown that stroke survivors experience spasticity [14], excessive co-activation [15], and limited voluntary activation of finger muscles [16]. These deficits lead to difficulty in creating proper grasp postures [7] and delays in grip initiation and termination [17].

Thus, neural activation patterns present a prime target for therapeutic training, but this may require specialized technology. Unlike movement or force, clinicians are unable to directly

measure neural activity through observation or touch. A number of studies have investigated the use of EMG [41-42] or EEG [43-48] or EMG for stroke rehabilitation. While results have been promising, there are limitations to each approach. The EEG signals are typically used to create a brain computer interface (BCI) that the user manipulates through mental imagery, such as to create ERD or ERS. Without actual movement, however, the ERD may not represent excitation of descending corticospinal pathways as needed for stroke therapy [49]. Movement, however, typically corrupts the EEG signal. Conversely, EMG signals are unable to capture movement preparation and initiation.

A system incorporating both EEG and EMG feedback may allow training throughout the movement and examination of both the central and peripheral nervous systems. We have developed such a system, which includes neural control of an active hand exoskeleton. Use of a robotic device in conjunction with the neural training permits proper movement to be associated with generation of task-appropriate neural activation patterns to facilitate a type of Hebbian

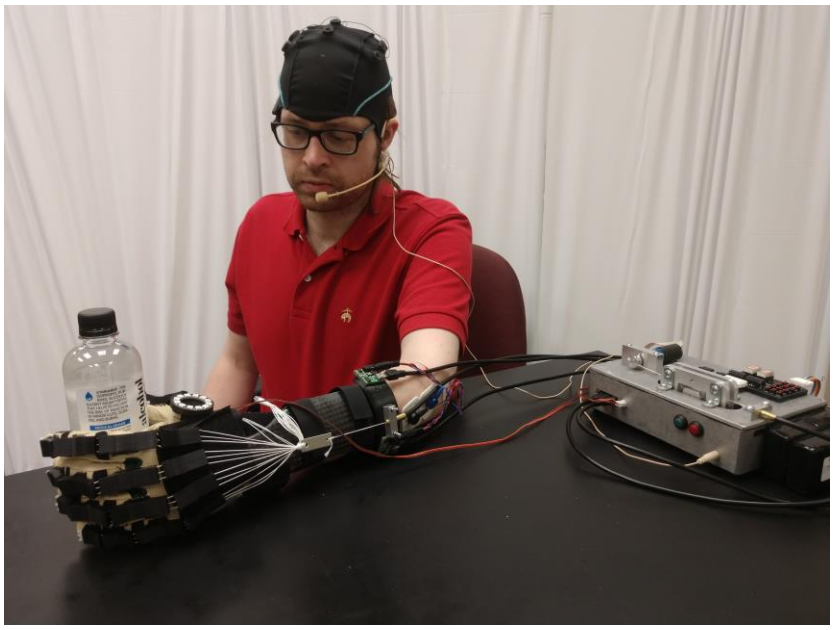

Figure 2.1 Complete EEG and EMG-controlled hand exoskeleton system. Components include a control box, an actuated glove, an EEG cap, a headset microphone, and two EMG boards.

learning [50]. The system has the capability to train both types of signals, together or in isolation, with or without the hand exoskeleton.

To evaluate system performance, we conducted a pilot study with 5 neurotypical participants. We hypothesized that the participants would be able to successfully operate the system within the course of a single session and would show improved control over the course of training as evidenced by faster task completion times.

2.2 System Design

2.2.1 Components

The developed system (**Fig. 2.1**) enables independent or integrated practice of control of EEG and EMG signals. By design, a variety of EEG systems may be used with the system. The EEG signals are processed in real-time using the BCI2000 [51] platform which derives a BCI control signal from a weighted linear combination of spatio-spectral sensorimotor rhythm (SMR) feature amplitudes. The BCI2000 environment is used to create different training scenarios and provide visual cues and real-time feedback to the user.

EMG signals are recorded from desired muscles using passive electrodes and processed with a custom printed circuit board (PCB). The PCB bandpass filters the EMG signal between 20-450Hz, applies a variable gain (G = 500, 2000, 8000), full-wave rectifies the signal, and creates an activity envelope using a 10Hz lowpass filter. The non-rectified signal is also available for analysis. The processed EMG signals can be transmitted to the BCI2000 environment for display. Alternatively, EMG amplitude can be represented with an LED ring (NeoPixel Ring, Adafruit) attached to the distal upper extremity so that the user can maintain eye contact with the hand and still receive feedback.

EEG and/or EMG signals can be used to drive the VAEDA Glove, a one degree-of-freedom device which uses cable-driven actuation to assist extension and resist involuntary flexion of all five digits simultaneously. A servomotor (Faulhaber, Inc.) mounts to a fixed control box (**Fig. 2.2**, left) and drives a pulley around which the cable (Spectra kite line, Windstar Kites) is wound. The cable passes through a custom-built load cell assembly for measuring cable tension and along a Bowden conduit that guides the cable from the control box to the hand exoskeleton (**Fig. 2.2**, right). The distal end of the cable connects to a set of 5 cables, one for each digit. Each cable in turn splits into 3 separate cables that traverse through 3D-printed cable guides affixed to a modified leather glove. The cable guides serve to increase the moment arm at each joint, preclude cable rubbing across the joint, and prevent joint hyperextension. The three cables provide greater lateral (radial-ulnar) stability than a single cable.

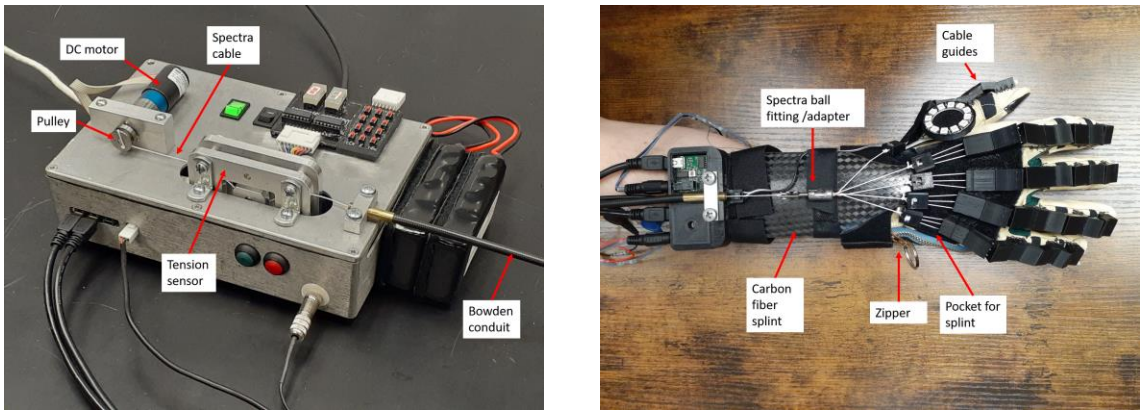

Figure 2.2 Components of hand exoskeleton. (Left) Cable is attached to a DC motor through a pulley. The cable traverses through a tension sensor which measures force and into a Bowden conduit. (Right) Distal end of Bowden conduit attaches to a carbon fiber splint that is secured to forearm with hook-and-loop fasteners. Single cable splits into 15 separate cables (3 per digit) which apply torque to the finger joints via 3D printed cable guides.

An Arduino Due microcontroller with a custom printed circuit board (PCB) controls the VAEDA Glove by providing output command signals to the servomotor via an H-bridge motor driver IC. The device is powered by two 7.4V LiPo batteries making it portable, a desirable

feature for busy rehabilitation clinics. From past experience working with the VAEDA Glove, the device can be used continuously for up to one week before needing to be recharged.

2.2.2 Control

We developed a custom graphical user interface (GUI) in MATLAB (**Fig. 2.3**) to coordinate collection of EEG and EMG signals and control of the VAEDA Glove exoskeleton. The communication flow diagram is shown in **Fig. 2.3**. The MATLAB GUI communicates with BCI2000 using a COM server-client interface to send high-level commands, such as "Start" and "Stop," as well as subject-specific parameters. Additionally, the MATLAB GUI communicates with the Arduino Due using a USB serial interface. Depending on the selected therapy mode, the Arduino Due can be configured to relay data back to the MATLAB GUI directly or to establish a connection with BCI2000 using a UDP protocol. This setup allows us to control the glove while not interrupting real-time signal processing and neurofeedback.

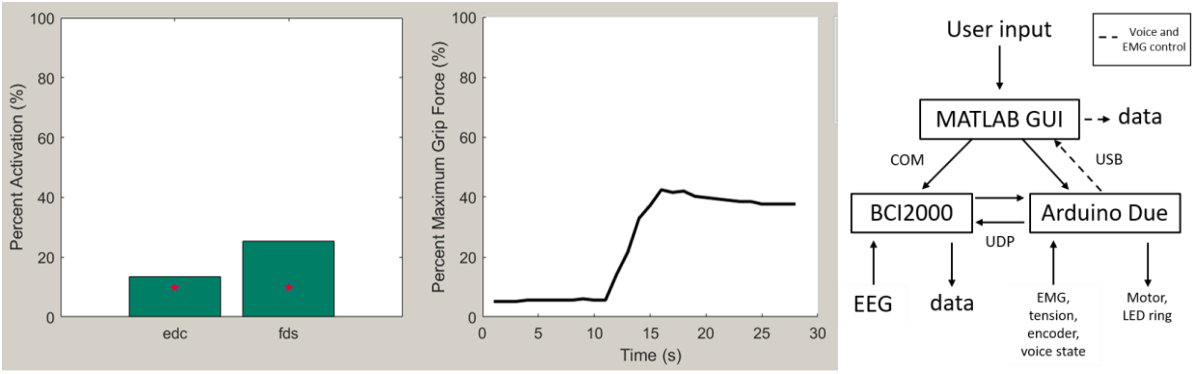

Figure 2.3 MATLAB GUI and communication flow diagram. MATLAB GUI (left) provides user-friendly interface for therapist to select operating mode of exoskeleton, record EMG activations and force for maximum voluntary contractions, and load in subject-specific parameter files for BCI2000. Communication flow diagram (right) shows the various inputs and outputs as well as the communication protocols that enable the therapist to use the MATLAB GUI to coordinate the Arduino Due and BCI2000.

In scenarios of self-paced functional task practice, voice commands can also be used to control the VAEDA Glove. We have found this to be an effective means to selecting movement state (e.g., "open", "close", "hold"). Voice commands are captured by a headset-mounted

microphone (B3 Countryman) and are processed by a voice recognition board (SR-07 Images SI) inside of the control box. Once the state is known, EEG/EMG signals can be used to drive the desired movement. The GUI can also select among different VADA Glove operating modes. For example, we have implemented a new impedance controller to provide the user haptic feedback when interacting with virtual objects. We use a high-gain inner force feedback loop to allow the servomotor to behave as a virtual spring despite its high gear reduction and low backdrivability.

2.3 Device Evaluation Study

2.3.1 Study Design

We recruited neurologically intact participants for a pilot study to evaluate system performance. Right-handed young adults with no history of neurological disease, orthopedic impairment or pain of the hand preventing movement, or visual impairment were eligible for the study. All participants provided written informed consent. This study was approved by the Institutional Review Board of North Carolina State University.

2.3.2 Protocol

For the entirety of the experiment, subjects sat comfortably in front of a television monitor placed at eye level. Their right forearm and hand rested on a side table in a posture of neutral pronation/supination with the elbow flexed 90°. The VAEDA Glove, which maintained the wrist in neutral flexion/extension, was placed on their right hand.

Participants first completed a BCI calibration phase consisting of 3-5 runs with 8 trials per run. One-minute rest breaks were provided between runs. Trials were separated by a 20-second inter-trial interval and a one-minute rest break was provided after each run. Each trial consisted of a two-second *Relax* period during which the participant rested, followed by a one-second *Warning* period, in turn followed by a *Cursor* period (**Fig. 2.4**). During the *Cursor* period, a cursor would appear at the left edge in the middle of the screen and move toward a target at the bottom right edge of the screen with a constant velocity. Participants were instructed to prepare for hand opening while they passively watched the cursor. Once the cursor reached the target, participants performed a grasp-and-release task with the VAEDA Glove. They opened the hand to the Glove extension limit, flexed the fingers around a virtual ball (rendered through haptic feedback from the Glove), held a submaximal grip force on the ball for one second, and then opened the device to full extension. Subjects used voice commands to control the movement direction (flexion/extension) of the VAEDA Glove and EMG signals from extensor digitorum communis (EDC) and flexor digitorum superficialis (FDS) to drive movement in the chosen direction. FDS had to exceed a specified threshold and EDC had to be below a certain threshold for digit flexion to occur, while the opposite criteria had to be achieved for digit extension.

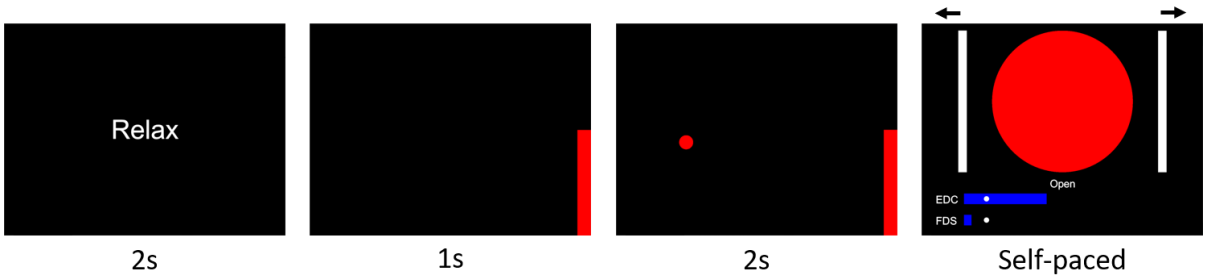

Figure 2.4 EEG-EMG+Voice Task. The subject first used motor imagery to modulate the SMR rhythm and control the vertical velocity of a cursor moving with a constant horizontal velocity from the left edge of the window to the right edge. Progression to the movement phase was contingent on the subject successfully hitting a target that occupies the bottom 50% of the window. Once the target was hit, the subject was presented a new screen which displayed the VAEDA Glove aperture as two white vertical bars that simultaneously moved inward or outward to represent a virtual compliant ball, the current Glove direction as set by voice command, and the FDS and EDC EMG signals (blue horizontal bars indicate signal amplitude and white dots indicate associated thresholds).

Failure to meet these requirements resulted in the device maintaining the current posture. Thresholds (typically around 10%) were set as a percentage of the signals recorded during maximum voluntary contractions of each muscle.

Following parameterization of the BCI control signal from examination of the calibration data, the subjects repeated the same task as described, but additionally providing active control of the cursor during the *Cursor* period by modulating EEG signals. Participants controlled the vertical velocity of the cursor by increasing or decreasing the spectral power of a chosen EEG channel over selected frequency ranges. Progression to the EMG-controlled hand movement phase was contingent on the subject successfully hitting the target. Each participant completed 5 runs of 8 trials with a 20-second inter-trial interval. A one-minute rest break was provided after each run.

2.3.3 Data acquisition

EEG signals were acquired from 8 active electrodes placed on a fabric cap (actiCAP Classic, Brain Vision) in accordance with the international 10-10 naming system: F5, Fz, F6, C3, C4, P5, Pz, and P6. The reference electrode was placed at FCz, and the ground electrode was placed at AFz. Conductive gel was applied to reduce electrode impedance below 15kΩ. The signals were amplified and digitally sampled at 1000Hz using a BrainAmp DC amplifier (Brain Vision). The measurement range was set to +/- 3.28mV, providing a 16-bit resolution of 0.1μV. The signals were bandpass filtered between 0.016Hz and 250Hz and streamed from Brain Vision Recorder to BCI2000 using an RDA server-client interface.

EMG signals were acquired from the EDC and FDS muscles using adhesive passive electrodes. The ground electrode was placed on the lateral epicondyle of the humerus. The EMG signals were processed using the custom PCBs on the VAEDA Glove and then sampled by the

Arduino Due at 200 Hz, along with the servomotor encoder signal and the voice state. BCI2000 sub-sampled these signals at 25Hz for display and storage.

2.3.4 BCI Signal Processing

In order to parameterize the BCI control signal, we extracted features from the BCI calibration data that were predictive of relaxing vs. right hand movement preparation. This was performed offline using custom MATLAB scripts. We chose to focus our analysis on channel C3, which overlies the hand region of the contralateral sensorimotor cortex. We analyzed the EEG data recorded during the final one second of the *Relax* period and the final one second of the *Cursor* period for this electrode. EEGLAB's automatic epoch rejection algorithm was used to reject epochs that exceeded a probability threshold of three standard deviations. Amplitude spectra were computed from the remaining epochs using an FFT with a 0.4-second rectangular window and 50% overlap. Potential features consisted of spectral amplitude in 3Hz-wide frequency bins within the sensorimotor rhythm frequency range (i.e., 9-30Hz). We used stepwise linear regression in order to determine which feature(s) best predicted task condition. The tolerances for adding or removing features from the model were each set to p=0.05. BCI2000 was then configured with the selected features to be used for online cursor control during the *Cursor* period for the full control trials.

2.3.5 Data Analysis

In order to evaluate whether subjects were improving over the course of training, we performed statistical tests comparing the average task completion time and movement initiation latency for the first 8 trials to the last 8 trials successful trials (out of 40 total trials). Due to the small sample size (n=5), we performed the nonparametric Wilcoxon signed-rank tests to assess the impact of training phase on the outcome measures. Task success rate corresponded to BCI

classification accuracy as all participants were able to complete the movement portion of the trial following successful BCI operation. Therefore, we evaluated if task success rate was significantly above chance level (50% for a binary classification task) using an inverse binomial cumulative distribution function [52].

2.4 Results

A total of 5 subjects (4 male/1 female) between the ages of 21-28 participated in the study (**Table 2.1**). From the EEG signals, we were able to identify frequency bands for electrode C3, positioned over the contralateral sensorimotor cortex, which showed ERD prior to movement. The selected frequency bins varied across subjects. All five subjects used at least one feature in the beta band (13-30Hz) for BCI control and two subjects (C and D) additionally used a feature in the alpha band (8-12Hz).

We were also able to detect EMG signals from the chosen muscles and these were successfully used to control the glove. The EMG thresholds used were typically 10% for both EDC and FDS muscles. However, two subjects (C and D) found a threshold of 10% for the FDS muscle too challenging due to co-activation of the EDC muscle during hand closing, so the FDS threshold was lowered to 5% in these subjects.

All five subjects were able to complete the combined BCI-EMG-voice task with a success rate of at least 60%. According to a binomial distribution with 40 trials, an accuracy of at least 63% indicates that BCI control was significantly above chance level with $p<0.05$. This was

Table 2.1 Subject characteristics, task parameters, and task success rate. * indicates significance at $p<0.05$.

Subject	Age	Sex	SMR Frequency (Hz)	EDC, FDS Threshold (% MVC)	Task Success Rate (%)
A	20	M	24, 30	10, 10	63*
B	21	F	21	10, 10	60
C	21	M	9, 30	10, 5	68*
D	28	M	9, 18, 30	10, 5	63*
E	21	M	21	10, 10	73*
Average	-	-	-	-	65*

achieved by 4-out-of-5 subjects, and the change in accuracy was marginally insignificant for Subject B (p=0.057).

Fig. 2.5 displays the r^2 scalp topography averaged across subjects and the amplitude and the r^2 spectra for all five subjects individually during successful BCI trials. From the averaged r^2 scalp topography, we can see that BCI control was being driven by activity underlying channel C3, consistent with the SMR. As can be seen in the spectra plots, 4-out-of-5 subjects (A-D) generated ERD during successful BCI control. These data suggest that Subject E was using facial muscle activation to control the BCI (the power during motor imagery remained constant or even increased from 20-70 Hz). The spectra plot for Subject C suggests that even better performance might have been attained by focusing on the 18Hz frequency band for this subject.

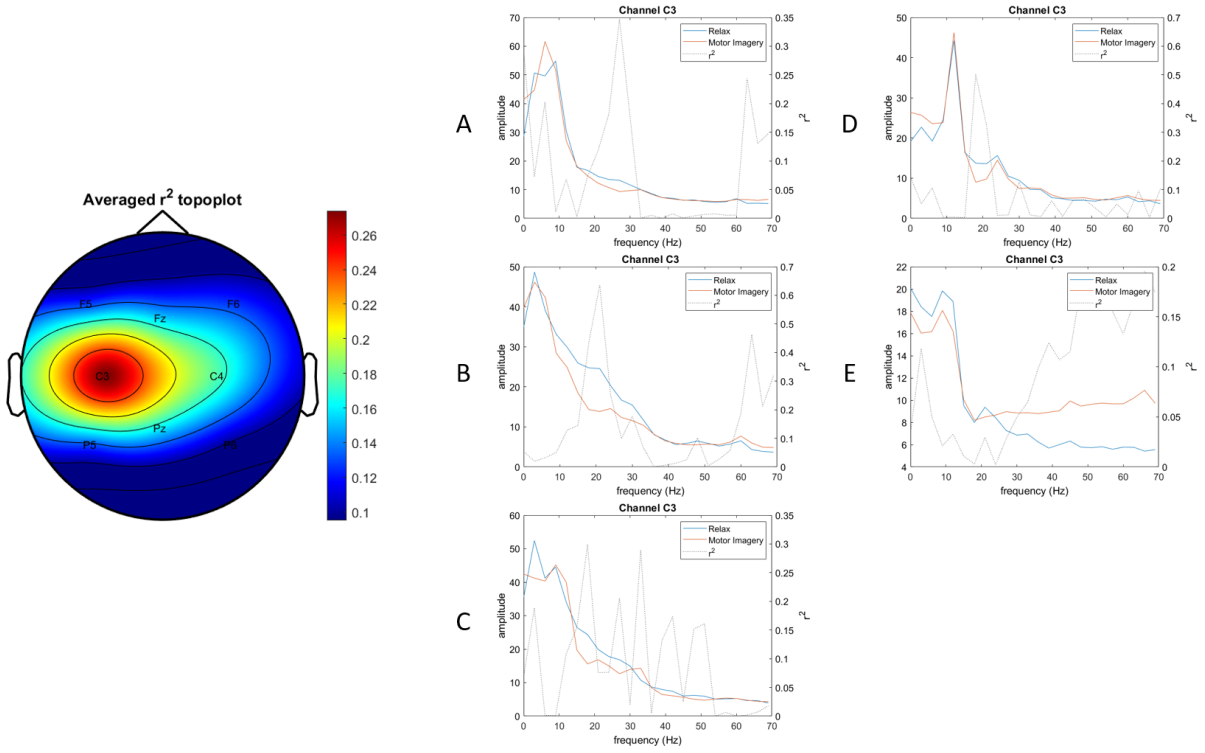

Figure 2.5 Sensorimotor rhythm control during BCI feedback. (Left) Scalp r^2 topoplot at subject-specific BCI control frequencies averaged over all five subjects. (Right) Amplitude and r^2 spectra for subjects A-E. Subject A-D demonstrated SMR-based BCI control. Subject E demonstrated facial EMG-based BCI control.

In general, subjects were able to integrate EEG, EMG, and the exoskeleton to achieve the task. For example, Subject A created ERD most prominently in the 24Hz frequency bin about 2.5 seconds prior to the cursor hitting the target (**Fig. 2.6)**. It should be noted that ERD was successfully generated using motor imagery rather than overt movement as both the FDS and EDC EMG signals remain zero during the BCI control period. This was subsequently confirmed for all 4 subjects who attained SMR-based BCI control. Upon the cursor hitting the target, Subject A increased their EDC activation above the EDC threshold value while keeping FDS relaxed and below the flexor threshold value, thereby driving the Glove into opening.

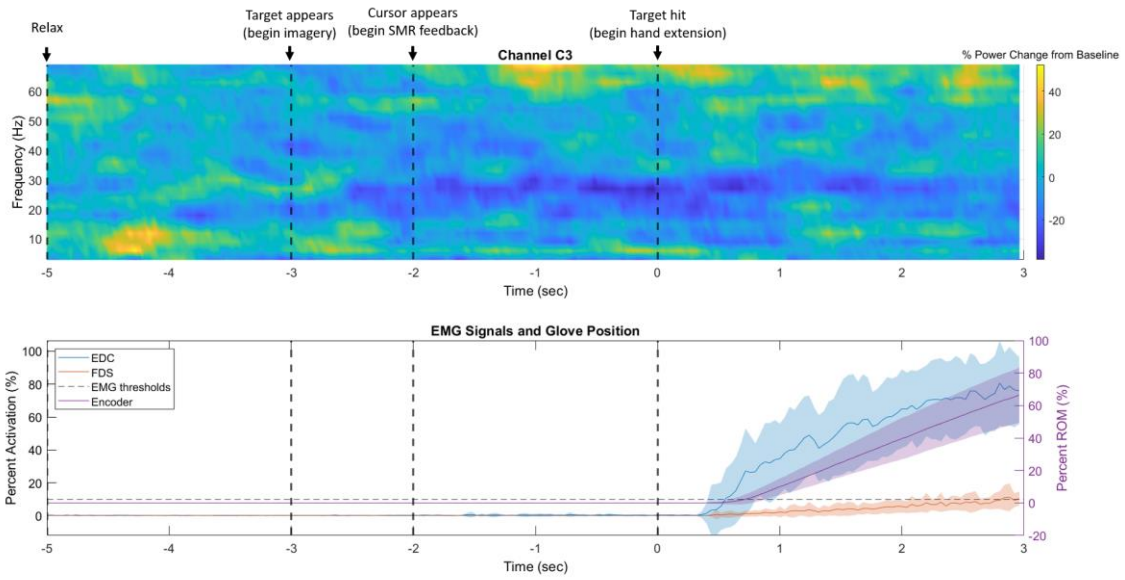

Figure 2.6 EEG, EMG, and position signals from Subject A. Showing transition from motor imagery-based BCI control to EMG control averaged across successful trials. (Top) ERD begins about 2.5s preceding the cursor hitting the target. Baseline is -4s to -3s. (Bottom) EDC activation begins to ramp up about 0.5s after the cursor hits the target, FDS activation stays below threshold, and glove begins to open.

Subjects were then required to use voice and EMG control to manipulate the VAEDA Glove to perform the desired task (**Fig. 2.7).** As can be seen, subject A, for example, was successfully able to activate his EDC muscle above the 10% MVC level while

maintaining his FDS muscle activation below the 10% MVC level thereby driving the glove open to the extension limit. The subject was then able to use a voice command to switch the Glove into the "close" state. The subject then deactivated/activated the EDC/FDS muscles below/above the threshold values to close the hand around the virtual object (generated by the VAEDA Glove). The subject then used another voice command to switch the device into the "open" state. Finally, the subject activated/deactivated the EDC/FDS muscles above/below the threshold values to open the Glove back to the extension limit.

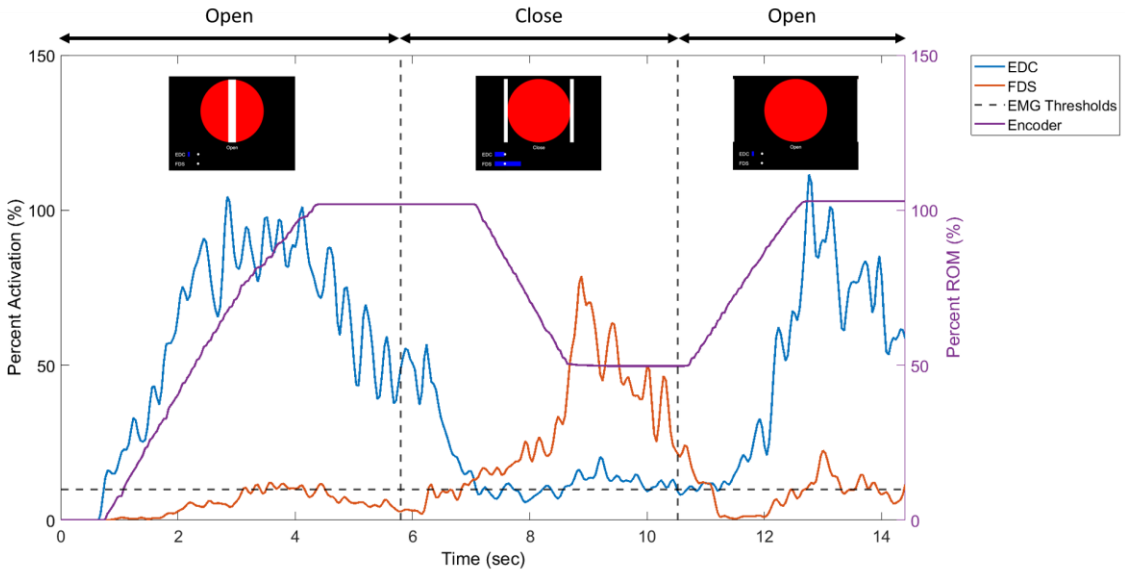

Fig. 2.7 Representative EMG and position signals from a single trial of Subject A. At time t=0, the glove is at the flexion limit with the two vertical white aperture bars in the center of the screen. The subject then activates the EDC muscle (blue trace) and above threshold and keeps FDS muscle (orange trace) below threshold in order to drive the glove open to the extension limit (purple trace). Once at the extension limit, at t=5.8s, the subject uses a "Close" voice command to switch the glove into the close state. He then deactivates EDC and activates FDS below/above the thresholds in order to close the glove onto the virtual object (red circle). After squeezing for approximately 2 seconds, the subject uses an "Open" voice command to switch the glove into the open state. The subject then activates/deactivates the EDC/FDS muscles above/below the thresholds to open the glove to the extension limit. Trials are ended manually by the experimenter upon task completion.

All five subjects reduced the time required to complete this task over the course of training (**Fig. 2.8**). The mean completion time for the last 8 trials was significantly smaller than the mean completion time across the first 8 trials according to the Wilcoxon signed rank test ($p < 0.05$, **Table 2.2**). The initiation latency for activating EDC above the threshold level once the BCI cursor hit the target also decreased for 4 of the 5 subjects for the last 8 trials in comparison to the first 8 trials (**Fig. 2.9**, **Table 2.2**), although this change was not significant across subjects ($p = 0.09$) despite a mean decrease of over 9% across subjects.

Table 2.2 Task completion time and latency.

Subject	Task Completion Time (s)		Latency (s)	
	First 8 Trials	Last 8 Trials	First 8 Trials	Last 8 Trials
A	23.58	21.96	0.77	0.72
B	19.76	17.96	1.45	1.08
C	22.17	20.49	1.14	1.00
D	19.63	18.25	0.68	0.75
E	25.73	25.70	1.17	1.02

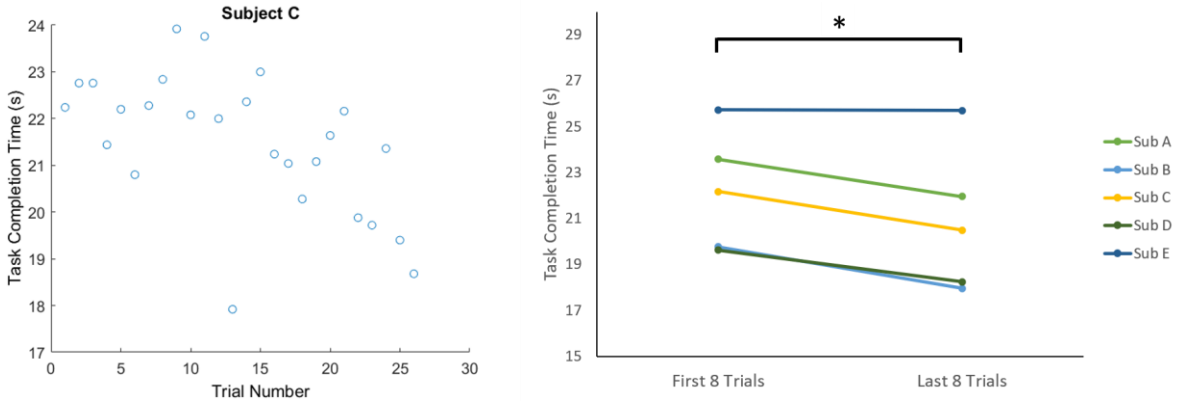

Fig. 2.8 Trial number vs. task completion time. (Left) Scatter plot of a representative subject (Subject C). (Right) All 5 subjects improved task performance over the course of the training session. * indicates significance at $p<0.05$.

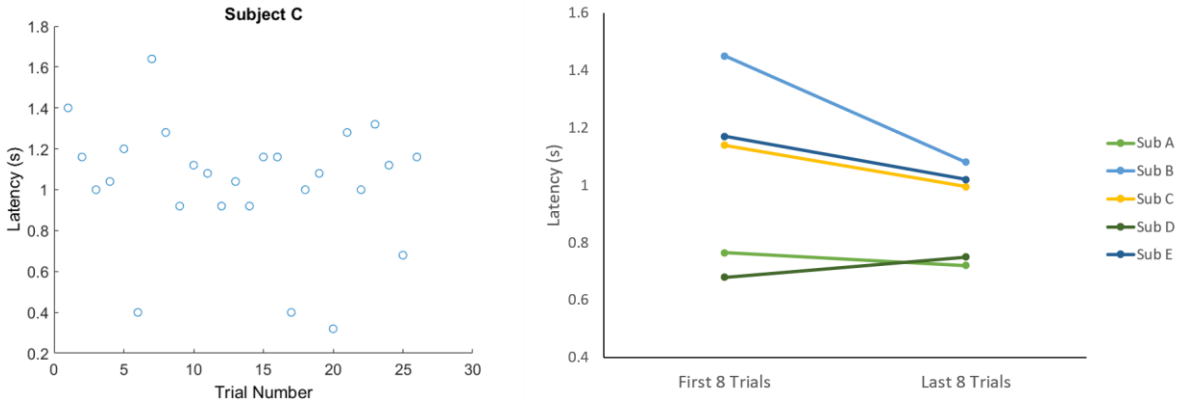

Fig. 2.9 Trial number vs. latency. (Left) Scatter plot of a representative subject (Subject C). (Right) All 4-out-of-5 subjects improved movement latency over the course of the training session.

2.5 Discussion

The novel rehabilitation platform we developed enables EEG and/or EMG control of a hand exoskeleton to facilitate rehabilitation by focusing on the neural activation issues underlying impairment. The integration of real-time EEG and EMG control with practice of a physical task, as assisted with the hand exoskeleton, enables the generation of proper sensory feedback associated with correct efferent commands. It has been found that BCI interventions that incorporate physical practice provide greater benefit than those that involve only visual feedback or passive movement [49,53].

The use of both EEG and EMG signals enabled targeted practice of neural control from pre-initiation to relaxation. While other investigators have incorporated both BCIs and EMG signals into the control paradigm, forming “hybrid BCIs” (hBCIs) [54-56], the primary goal of these systems is merely to use EMG to improve decoding of motor intent. In contrast, our system aims to directly train aberrant neural activation patterns that are present at both the cortical and muscular levels throughout the entire movement task. Bhagat et al. used an “EMG gate” to improve intent detection of a BCI classifier in order to drive an elbow exoskeleton in a study of

stroke survivors [56], but they did not require proper muscle activation patterns to be generated in order to initiate movement. Leeb and colleagues employed a similar control approach as our device, requiring ERD followed by EDC activation, in order to drive FES to stimulate finger extension in a single case study [54], they did not train aberrant EMG activation patterns throughout execution of an entire movement task. Sarasola-Sanz et al. used ERD to gate the movements of a 7 degree-of-freedom robotic exoskeleton whose speed and direction were partially determined by an EMG decoder [55]. However, they did not address the issue of involuntarily sustained flexor activation during object release.

In our device evaluation study, we demonstrated that neurologically intact individuals could learn to use sequential EEG-EMG control to perform a grasp-and-release task over the course of a single training session. Mean BCI classification accuracy (65%) was better than chance across subjects, although the power spectrum suggested that one subject may also have been using facial EMG signals to drive the BCI. While greater accuracy may be achievable with more advanced BCI algorithms [57], subjects in this study demonstrated an ability to learn to modulate ERD within a single session using only one electrode. We chose a simplified EEG montage to model what might be achievable in a clinical setting based on existing technology. However, as dry electrode systems improve, this system could easily be expanded to use more electrodes and take advantage of more advanced BCI algorithms.

Subjects were able to transition readily from EEG to EMG control. Subjects with initially poor movement latency were able to rapidly improve over the course of training. Only one subject who had initially good performance did not improve movement latency. Our results are in good agreement with a previous multi-session BCI study that found movement latencies of around 600msec and greatest improvements in individuals with initial poor performance [58].

Subjects were also able to reduce task completion time significantly. Interestingly, the one subject who had only marginal improvement used facial EMG rather than EEG to control the BCI. One previous study found that most subjects who controlled the BCI with facial EMG within the first BCI session were able to gain true ERD-based BCI control by the 10th training session [59].

Generalizability of results may be limited by the subject population. For this initial evaluation, five subjects used the system over a single session. This study was also conducted with a neurotypical population rather than stroke survivors. Because our participants were neurotypical, we were able to select channel C3 for BCI control based on the fact that it overlies contralateral sensorimotor cortex. With stroke survivors who may have experienced cortical reorganization throughout stroke recovery, we may need to consider other channel locations including those overlying the ipsilateral sensorimotor cortex [43,60]

Despite these limitations, we were able to show that the system performed as intended. Subjects were able to use the provided visual feedback of neural activity to control a hand exoskeleton to perform a task. Therefore, we believe that this successful proof-of-concept test in neurologically intact individuals merits further study in stroke survivors.

CHAPTER 3: TRAINING GRIP MUSCLE RELAXATION USING REAL-TIME FEEDBACK OF SENSORIMOTOR RHYTHMS

***Abstract*— We explored the use of a novel brain-computer interface (BCI) application using sensorimotor rhythm (SMR) feedback during isometric grip force production to train grip relaxation. A group of neurotypical participants was able to learn to control the BCI over five experimental sessions. Upper extremity task performance improved following BCI training. These results motivate the further exploration of this protocol for upper extremity rehabilitation in stroke survivors and individuals with Parkinson's disease.**

3.1 Introduction

Neural impairment is often associated with difficulty in activating motoneurons, but deactivating muscles may be challenging as well. Stroke survivors [14,17] and individuals with Parkinson's disease (PD) [61] may experience sustained involuntary activation of finger flexor muscles that may lead to difficulty releasing objects. The continued activation could also impair hand opening for subsequent grasps, especially as the flexor muscles are much stronger than the extensors. Delays in muscle deactivation result in difficulty completing activities of daily living [10].

It has been suggested that changes in intracortical inhibition following stroke [32,33] and PD [34,35] may play a role in prolonged activation of flexor muscles. EEG and MEG studies have found that event-related desynchronization (ERD) [24,36,62,63] normally precedes muscle relaxation. Within elderly individuals, this ERD was found to occur earlier than young individuals in spite of equivalent muscle relaxation latencies between the two groups [36]. Within elderly Parkinson's patients who have prolonged muscle relaxation, ERD is found to be significantly delayed relative to healthy age-matched controls [24].

Training of ERD, such as through a brain-computer interface (BCI), could thus potentially benefit grasp relaxation. Past studies of movement initiation showed that individuals could learn to modulate sensorimotor rhythms (SMRs) prior to movement when given feedback [58] and that this modulation could impact initiation delay and task performance [43]. Accordingly, we developed a BCI paradigm using motor imagery and BCI feedback to train modulation of SMRs associated with grasp release planning. In this study, we explored the impact of using this system in neurotypical young adults. We hypothesized that subjects could learn to control their SMRs during constant-force isometric grip and that down-regulation of pre-grip release SMRs would reduce the latency of grip muscle relaxation relative to up-regulation. We also hypothesized that the training would lead to improved hand task performance.

3.2 Methods

3.2.1 Study participants

We recruited n=10 neurotypical young adults (9 males) for this study. Participants were right-handed and at least 18 years old, with no history of neurological disease, orthopedic impairment or pain of the hand preventing movement, or visual impairment. All participants provided their written informed consent. This study was approved by the Institutional Review Board of North Carolina State University.

3.2.2 Protocol - Overview

During all five experimental sessions for each subject, we recorded their electroencephalographic (EEG) signals from bilateral sensorimotor cortical regions with a 32-channel active electrode cap (**Fig 3.1**). The reference electrode was placed at FCz, and the ground electrode was placed at AFz. The signals were amplified and digitally sampled at 1000Hz

using a BrainAmp DC amplifier (Brain Vision LLC). The signals were bandpass filtered between 0.016Hz and 250Hz and streamed from Brain Vision Recorder to BCI2000 [51] using an RDA server-client interface.

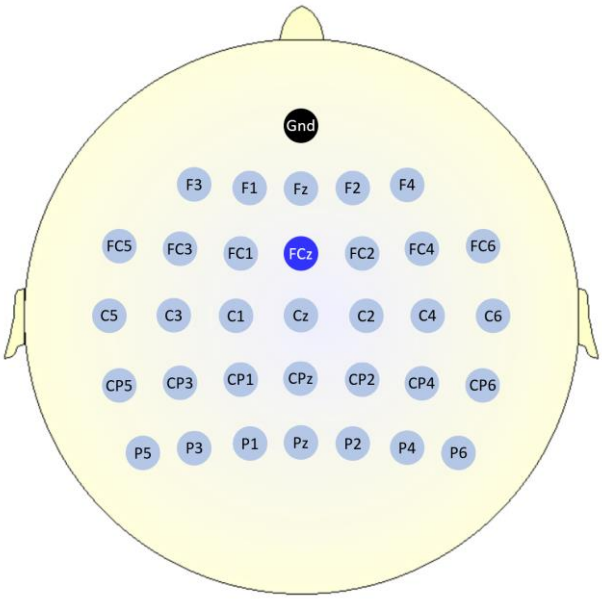

Figure 3.1 32-channel EEG layout. The electrodes overlay bilateral sensorimotor regions.

During Sessions 1 and 5, EMG signals were recorded from pairs of surface electrodes targeting extensor digitorum communis (EDC), flexor digitorum superficialis (FDS), and first dorsal interosseous muscles (FDI). The signals were amplified and bandpass filtered between 20-450Hz before being sampled at 1000 Hz by a DAQ device (USB-6001, National Instruments).

In each session, participants squeezed and released an electronic hand dynamometer (CAMRY with custom signal conditioning circuit board) with their right (dominant) hand while receiving visual feedback of grip force level presented on a television monitor from a custom BCI2000 application. Force data were sampled at 25Hz with an Arduino DUE and transmitted to the BCI2000 program controlling the visual display, along with the EMG data. A trigger pulse, generated by the Arduino DUE, initiated the DAQ sampling of the EMG signals and placed an event marker in the EEG data to enable data synchronization.

Each subject was asked to complete each of the five experimental sessions. Session 1 was a calibration session used to build the ERD-based release model and perform initial evaluations. Sessions 2-4 were training sessions during which the participant used motor imagery to modulate the SMRs for the chosen electrodes and frequency bands while maintaining isometric grip force. Session 5 consisted of final evaluations of BCI performance.

3.2.3 Session 1

In order to create a model of SMR, subjects performed a grasp release task (**Fig 3.2)**. At the beginning of each trial, subjects were asked to increase their grip force to 20% of maximal voluntary grip force and to maintain that level for 2 seconds. Visual feedback was provided in terms of a green circle indicating their current force level and a force target box corresponding to 20% +/- 3% of maximum voluntary grip force. Once the force level is properly maintained for 2 seconds, the participant enters a *Warning* period, during which the green circle turns either blue or yellow for 2 seconds, with a 50% probability for either condition. A yellow circle indicates that the subject should prepare to release their grip while a blue circle indicates that the subjects

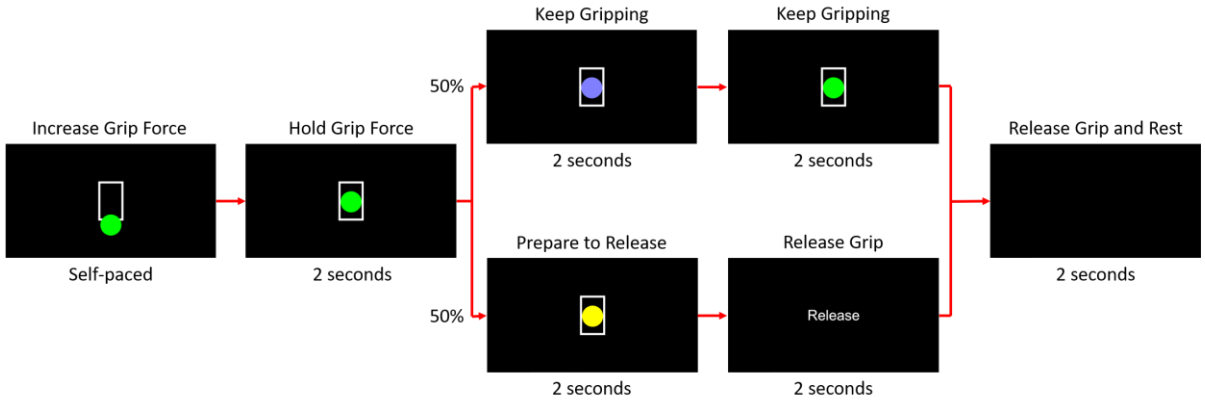

Figure 3.2 Session 1 BCI calibration task. At the beginning of each trial, participants must first increase their grip force and hold a green circle inside of a white force target box for 2 seconds. Once achieved, the circle turns blue or yellow, with a 50% probability for each, for 2 seconds. Blue circles warn that participants will the maintain grip in the following imperative period while yellow circles warns that participants should prepare to release their grip as quickly as possible in the following imperative period. Subjects then perform the previously instructed motor act over a 2-second interval. The screen then goes blank for 2 seconds and subjects relax their grip if not done so already.

will maintain their grip. Correspondingly, during the following *Imperative* period, subjects are instructed to either release the grip force as quickly as possible or maintain the same grip force. Trials are aborted if subjects move outside of the force target box during the *Warning* or *Imperative* periods. Participants rested for 2 seconds between successive trials. They performed nine runs of 20 trials with rest breaks of 1-2 minutes between runs.

3.2.3.1 Evaluations

To assess if the training regimen had any impact on upper extremity dexterity, we had subjects perform the Box & Block Test (BBT). The BBT is a standard metric to assess hand and arm dexterity in stroke survivors. Subjects used the right upper extremity to move as many blocks as they could from the right compartment of the box, over a divider, and into the left compartment of the box in a 1-minute period [64].

Subjects also performed a grip muscle relaxation latency evaluation task, as shown in **Fig. 3.3**. To begin each trial, participants were again required to increase their grip force to 20% of their maximum voluntary grip force and maintain that level for 2 seconds. Visual feedback of actual and target forces was again provided as described previously. If the force were produced correctly, the *Warning* period began, during which the circle turned yellow for a random period of 2-5 seconds. If subjects moved outside of the force target box during the *Warning* period, the trial was aborted and they received a text cue of "TooEarly." If the force requirement was met

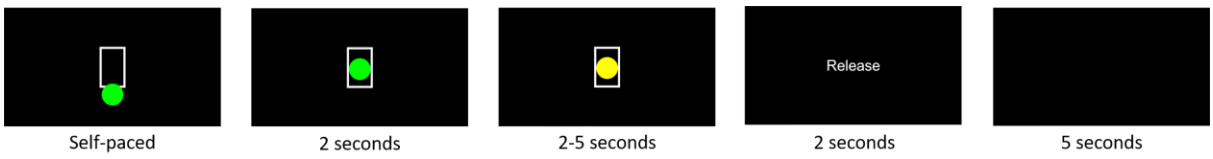

Fig. 3.3. Grip muscle relaxation latency evaluation. At the beginning of each trial, participants must first increase their grip force and hold a green circle inside of a white force target box for 2 seconds. Once achieved, the circle turns yellow for a random period of 2 to 5 seconds warning participants to prepare to release their grip as quickly as possible in the upcoming imperative period. Participants are then given a textual "Release" cue and must release their grip as quickly as possible. Following the "Release" cue, the screen goes blank for 5 seconds.

for the entire *Warning* period, then the *Imperative* period began and participants received a "Release" cue. Subjects were instructed to stop squeezing as quickly as possible while relaxing all hand muscles, including the extensors, as soon as they saw the "Release" cue. Participants rested for 5 seconds after each trial. They performed one run of 5 trials and one run of 10 trials, with a rest break of one minute between runs.

3.2.4 EEG data modeling

Following session 1, the EEG data were analyzed offline in order to parameterize a BCI controller used for the remaining sessions. We first removed the mean and re-referenced all EEG channels to a common average reference. We then extracted epochs corresponding to the final 1 second of the *Warning* cue in order to find features that best separated the yellow circle class (grip release preparation) from the blue circle class (keep gripping).

In selecting potential BCI control channels, we first considered a functional MRI study that identified activation primarily in contralateral primary motor cortex (M1), contralateral dorsal premotor cortex (PMd), and bilateral supplementary motor areas (SMA) during an isometric pinch relaxation task [21]. We then cross-referenced this with two EEG studies showing ERD preceding muscle relaxation with a clear contralateral predominance in central and frontocentral leads [36,63]. Thus, we focused the following subset of EEG channels for BCI control: FC3, FC1, C3, and C1. These channels overlie contralateral M1, PMd, and SMA [65]. Neighboring channels were only considered if this subset failed to show clear ERD.

We then computed amplitude spectra for each channel of interest and each epoch by fitting a 100^{th}-order autoregressive model [66] to 0.4-second windows and applying Welch's method of periodogram averaging with 75% window overlap. Features corresponded to the spectral amplitude of 3Hz-wide frequency bins within the range of the sensorimotor rhythm (9-

30Hz) for each of these channels. We then used a stepwise multiple linear regression procedure to add or remove features from the model predicting class label as +1 (for blue circles – maintain grasp) or -1 (for yellow circles – prepare to release). Inclusion and exclusion criteria for the regression model were each set to $p<0.05$.

3.2.4 Sessions 2-4

In sessions 2-4, subjects underwent BCI training by performing various mental imagery tasks while maintaining specified level of grip force. To begin each trial, participants were instructed to increase their grip force to 15% of maximum force in order to maintain a green circle within a force target box with limits of 15% +/- 3% of maximum grip force (**Fig. 3.4**). If the subject were able to hold the force for one second, the application would transition into the *Mental Imagery* period. Subjects were instructed to clear their minds if the green circle turned blue or to imagine releasing the grasp if the cursor turned yellow. Following this 1-second period, the brightness of the circle was controlled by the BCI control signal in accordance with the mapping derived from the Session 1 data. For blue circles, subjects had to increase the amplitude of the selected features (ERS), while for the yellow circle subjects had to reduce the amplitude (ERD). Proper amplitude modulation turned the circles brighter while improper amplitude modulation caused the circles to dim. Upper and lower thresholds were defined such that the circle turned green if the correct threshold was attained or red if the incorrect threshold was exceeded. If neither threshold was reached within the 3-second BCI feedback period, then the trial was aborted. The upper and lower threshold values were initially set to 0.4 standard deviations above and below the mean control signal and were adapted every trial in order to make the BCI feedback task more challenging if the subject was successful or easier if the subject was unsuccessful. Trials were aborted if grip force was not properly maintained (the

green circle moved outside of the force target box). The screen then went blank for 2.5-seconds allowing subjects to release their grip and relax. Subjects performed nine runs of 20 trials for each of the BCI training sessions.

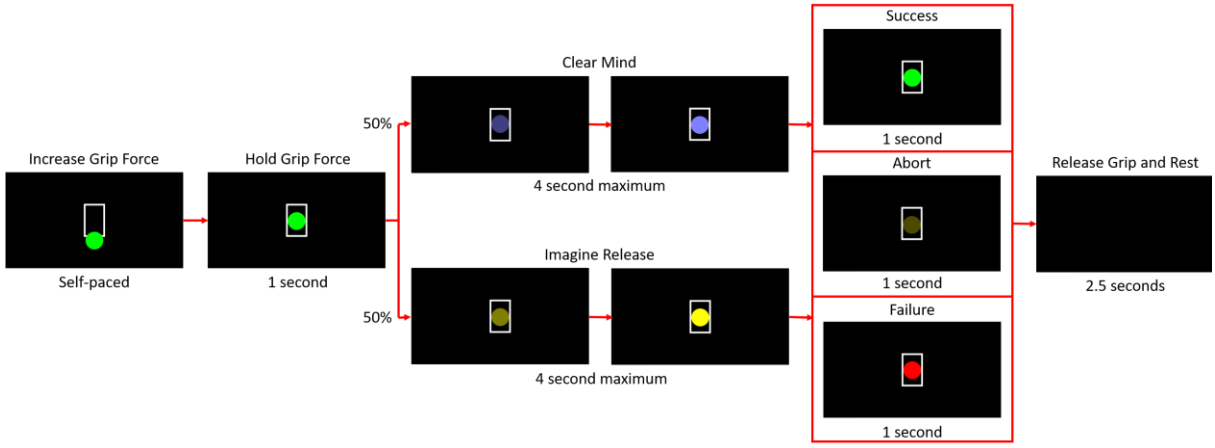

Fig. 3.4. Sessions 2-4 BCI feedback task. At the beginning of each trial, participants must first increase their grip force and hold a green circle inside of a white force target box for 1 second. Once achieved, the circle turns a dim blue or yellow, with a 50% probability for each, for 1 second. Blue circles instruct participants to begin clearing their minds, and yellow circles instruct participants to begin imagining grip release. Proper modulation of BCI control features caused the circles to brighten, while improper modulation caused the circles to dim. If the appropriate threshold was reached, the bright circles would turn green. Conversely, if the inappropriate threshold was reached, the dim circles would turn red. If neither threshold was reached within a 3-second period the trial would be aborted. The screen then goes blank for 2.5 seconds and subjects relax their grip.

3.2.5 Session 5

Subjects again performed the BBT and grip relaxation test as described for Session 1. Additionally, an evaluation was performed to determine the impact of SMR up-regulation and SMR down-regulation on grip release. Subjects maintained a grip force equivalent to 20% of maximum force for one second (**Fig. 3.5**). Subjects then performed the motor imagery-driven BCI feedback task as described previously. If the trial was successful, then there was a 50% likelihood that subjects would be required to release the grip as quickly as possible and a 50% likelihood that subjects would need to maintain the same level of grip force for an additional 2 seconds. Randomness in the outcome of successful trials was implemented in order to prevent subjects from anticipating an upcoming grip release cue which could have biased the results. If the trial was a failure or aborted, then subjects received the corresponding feedback as in

Sessions 2-5. After each trial, subjects released the grip if they had not already done so and rested for a 3-second inter-trial interval. Subjects performed nine runs of 20 trials.

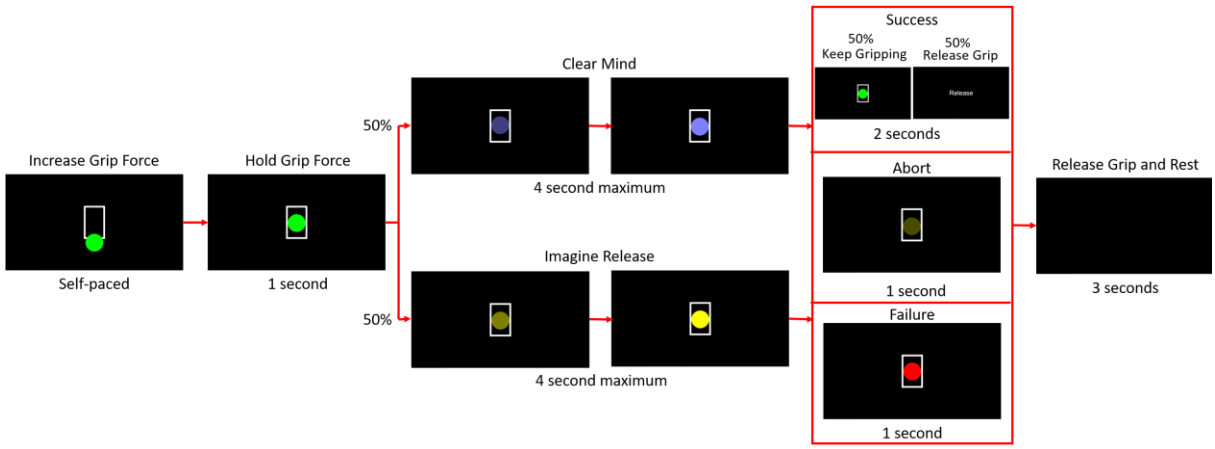

Fig. 3.5 Session 5 BCI evaluation task. At the beginning of each trial, participants must first increase their grip force and hold a green circle inside of a white force target box for 1 second. Once achieved, the circle turns a dim blue or yellow, with a 50% probability for each, for 1 second. Blue circles instruct participants to begin clearing their minds, and yellow circles instruct participants to begin imagining grip release. Proper modulation of BCI control features caused the circles to brighten, while improper modulation caused the circles to dim. If the appropriate threshold was reached, the bright circles would either turn green for 2 seconds (indicating that the participant should maintain the current force level) or disappear to reveal a textual "Release" cue for 2 seconds. Conversely, if the inappropriate threshold was reached, the dim circles would turn red. If neither threshold was reached within a 3-second period the trial would be aborted. The screen then goes blank for 3 seconds and subjects relax their grip.

Grip muscle relaxation was quantified by analyzing the FDI EMG signal, which had better signal-to-noise ratio than FDS. For each trial, we first removed the mean of the signal, applied rectification, and applied at zero-phase second-order Butterworth low-pass filter with a -3dB cutoff frequency of 10Hz [17]. We then computed the moving average across a 0.5-second data window and took the window producing the lowest mean value as the *baseline* (**Fig. 3.6)**. The *threshold* was defined as the mean plus three standard deviations of the *baseline*. We considered the first time point in which the moving average fell below the *threshold* to be the point at which muscle relaxation had occurred. The latency was defined as the time elapsed

between the presentation of the “Release” cue and the muscle relaxation time point. The average of the ten fastest trials was used as the latency for each condition.

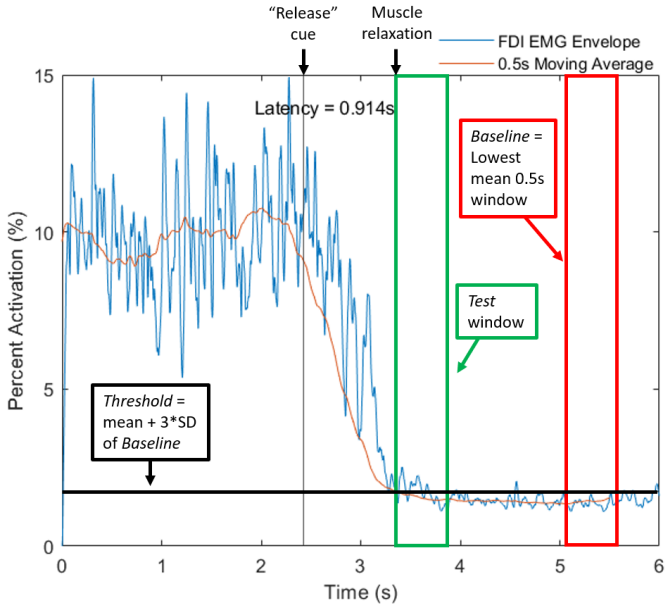

Fig. 3.6 Grip termination latency. Blue trace shows FDI EMG envelope for a single trial. We first determine the *threshold* for EMG relaxation by sliding a 0.5s window across the trial and selecting the window with lowest mean (*baseline*). *Threshold* is then set to lowest mean window plus 3 standard deviations of the lowest mean window. We then slide a 0.5s *Test* window over the data and consider muscle relaxation to occur at the first time point that the mean of the *Test* window decreases to below *threshold*.

3.2.7 Statistical Analysis

We first tested whether or not the BCI controller was performing significantly above chance level during the BCI evaluation of Session 5 [52]. We did this by computing the true positive rate as the number of correctly classified trials divided by the total number of trials in which a classification decision was made, i.e., aborted trials were excluded. Assuming that classification errors follow a binomial cumulative distribution, we computed a theoretical threshold for the true positive rate above which the results can be considered statistically significant. Additionally, we tested whether BCI performance was improving over the course of training by comparing mean BCI classification accuracy from Session 2 to Session 5 using a paired t-test. To examine the effect of training on hand task performance, we compared the BBT scores of Sessions 1 to those of Session 5 using a paired t-test.

We also tested the impact of SMR amplitude on grip relaxation latency. To do this, we compared the SMR amplitude during the blue and yellow circle *BCI feedback* periods of successful Session 5 trials in which participants received the "Release" cue. We compared the blue and yellow circle SMR amplitude and latency of the fastest 10 trials for each participant using a paired t-test.

Tests of normality were performed for the paired differences constituting the paired t-tests by examining the Shapiro-Wilk test. Evidence of non-normality would lead to use of Wilcoxon signed-rank test rather than a paired t-test.

3.3 Results

From the BCI calibration procedure from Session 1, we were able to successfully identify ERD associated with muscle deactivation and fit regression models that predicted grip release planning ($p<0.05$) in 9 out of 10 subjects (**Table 3.1**). The features selected for the models were exclusively drawn from the beta band (13-30Hz). Channel FC3 was the most frequently selected electrode for BCI control. As subjects F and G displayed ERD more strongly slightly anterior to the initial region of interest, we additionally considered features from channel F3 for these subjects. For subject H, we were not able to clearly identify ERD associated with grip release planning. Therefore, we selected channel FC3, 27Hz as this subject's BCI control feature with the expectation that he would be able to learn to modulate this feature with BCI training. This particular feature was chosen because it was the most frequently identified feature for other participants.

On average, participants performed the BCI task significantly above chance level at $p<0.05$ by Session 5 (**Table 3.1**). Notably, one participant (subject A) utilizing a single feature of FC1, 24Hz was able to obtain BCI control with a Session 5 accuracy of 79%. Subjects were able to improve their BCI performance over the course of training; BCI accuracy was significantly higher in the final evaluation in Session 5 relative to the initial BCI training in Session 2 ($p<0.05$, **Fig. 3.7**).

Table 3.1 Session 5 BCI evaluation task.

Subject	Channel	Frequency (Hz)	Channel	Frequency (Hz)	Session 5 Trials (Correct/Total)	Session 5 Accuracy (%)
A	FC1	24	-	-	83/105	**79.05**
B	FC3	18	-	-	65/115	56.52
C	FC3	27	C1	21	65/105	**61.9**
D	FC1	30	-	-	83/143	**58.04**
E	FC3	27	-	-	68/104	**65.38**
F	F3	27	FC1	21	59/92	**64.13**
G	F3	24	-	-	50/107	46.73
H	FC3	27	-	-	66/113	**58.41**
I	FC3	18, 21	-	-	44/93	47.31
J	FC3	30	-	-	58/120	48.33
Average	-	-	-	-	64/110	**58.43**

Bold indicates classification significantly above chance level.

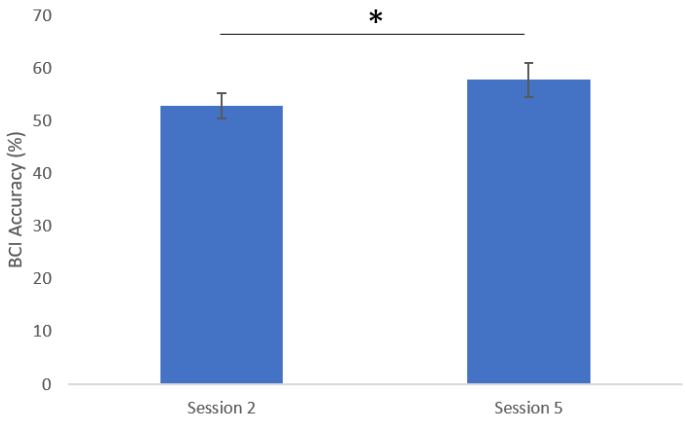

Figure 3.7 BCI accuracy over sessions. * indicates significant difference at $p<0.05$.

We further examined SMR modulation in Session 5 across electrodes and frequency bands for the successful BCI feedback trials (**Fig. 3.8**). As can be seen in the scalp topographies, the highest correlation values typically appeared localized to the electrode being used for BCI control. Furthermore, inspection of the channel spectra reveals sharp negative correlation peaks at the BCI control frequency, thereby indicative of true SMR-based BCI control (ERD associated with grip relaxation).

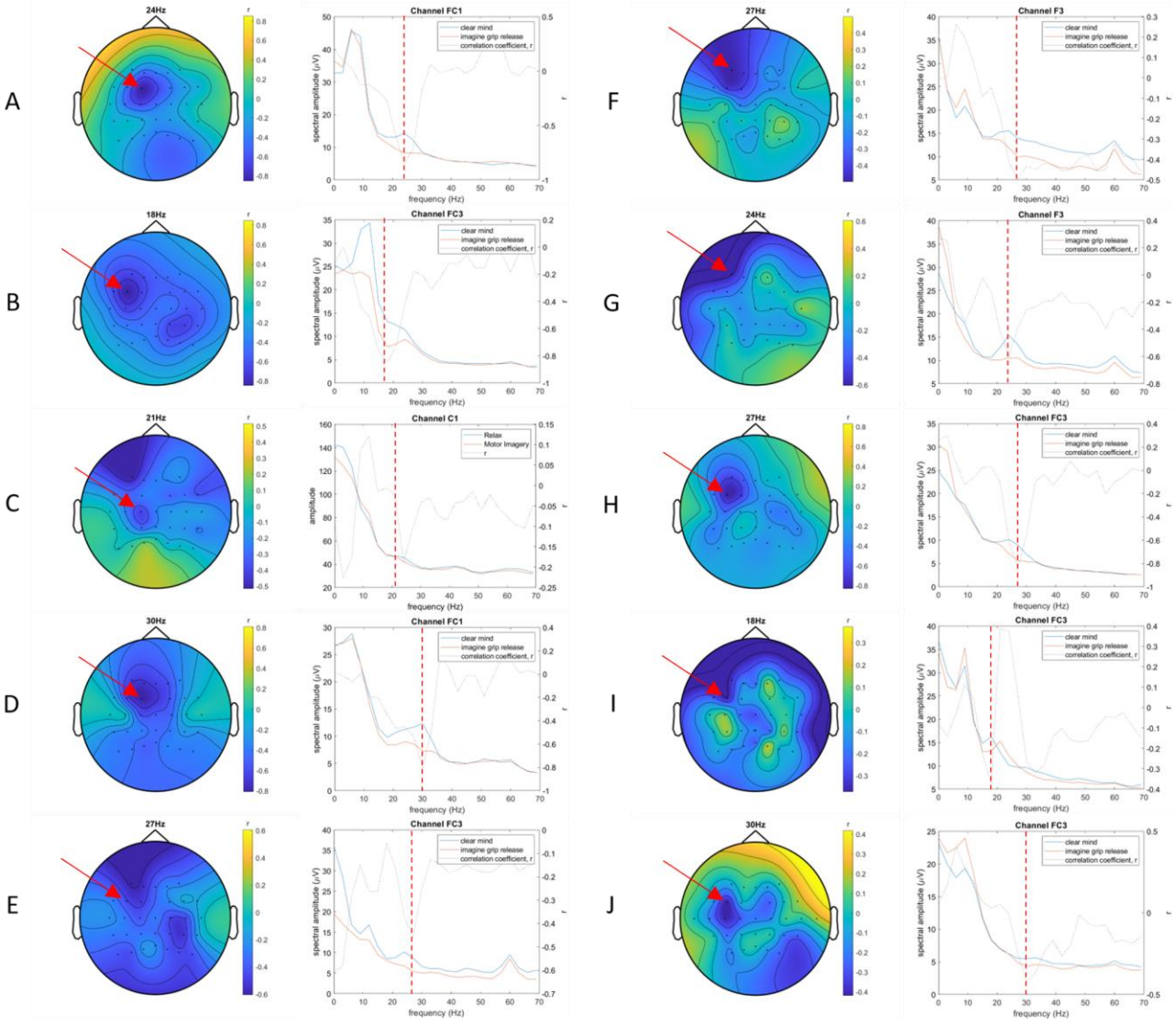

Figure 3.8 Session 5 scalp topographies and correlation spectra for successful BCI trials. Spatially- and spectrally-localized correlation values demonstrates true SMR-based BCI control.

We further investigated the BCI trials to determine if classification accuracy could potentially be improved with an alternative set of channel locations and frequencies. In consideration of data from all Session 5 trials, we observed that the features most strongly correlated with task condition typically differed from those used for the on-line BCI control, as found from the calibration in Session 1 (**Fig. 3.9)**. The most predictive channels were C1 and FC1, with 24Hz being the most frequently identified frequency band. Therefore, the introduction

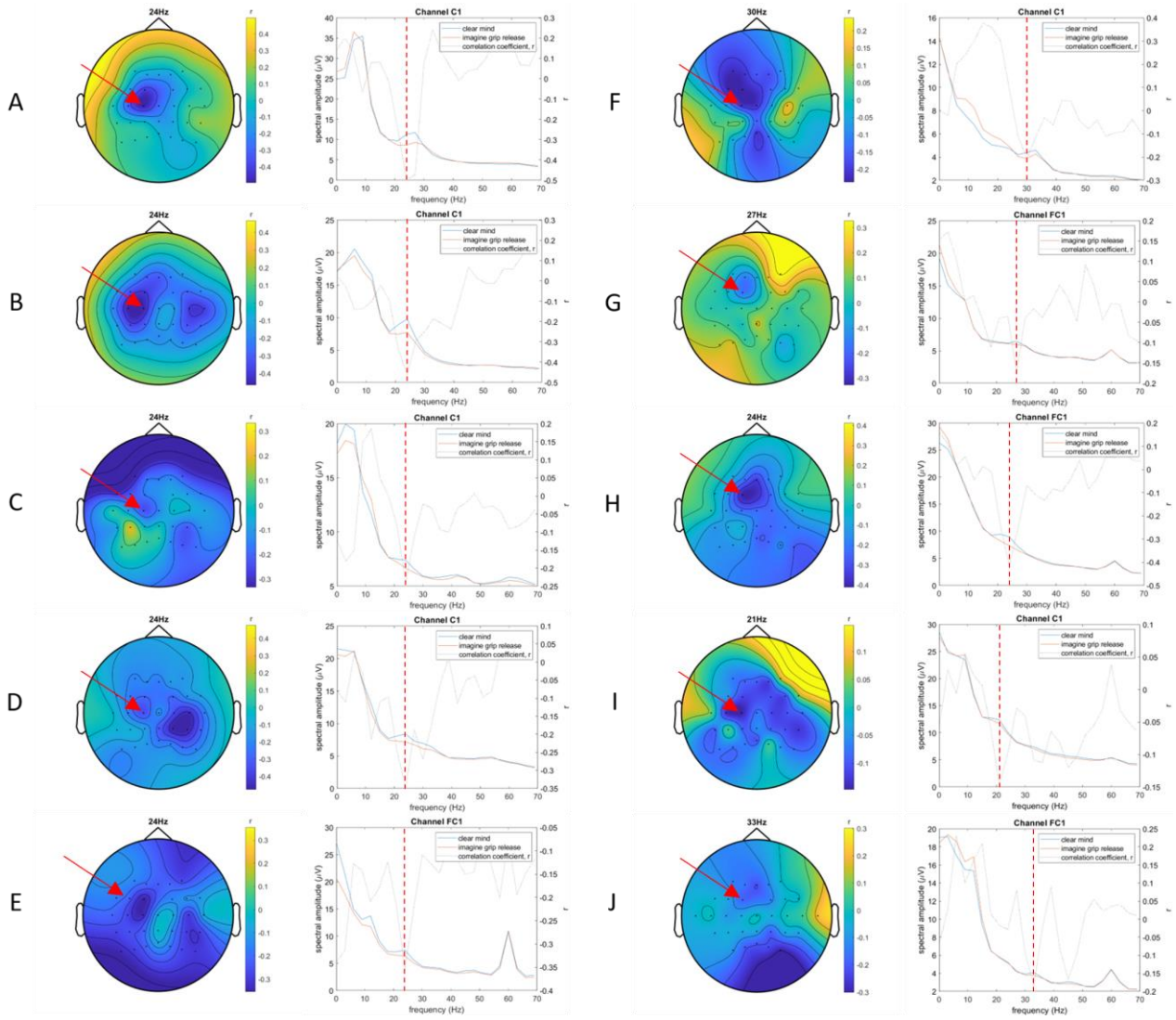

Figure 3.9 Session 5 scalp topographies and correlation spectra for all BCI trials. The optimal configurations for ERD differed from the ones selected for the BCI training. As expected, larger correlation values at the channel and frequency selected for BCI control coincided with better BCI accuracy.

of mental imagery and visual feedback shifted the region of peak ERD towards the midline. In three of the four subjects who did not exhibit BCI control above chance levels, we found sharp correlation peaks localized to channel FC1 and C1 in the lower gamma (31-49Hz) frequency band (**Fig. 3.10**), in addition to the peaks found in the beta band.

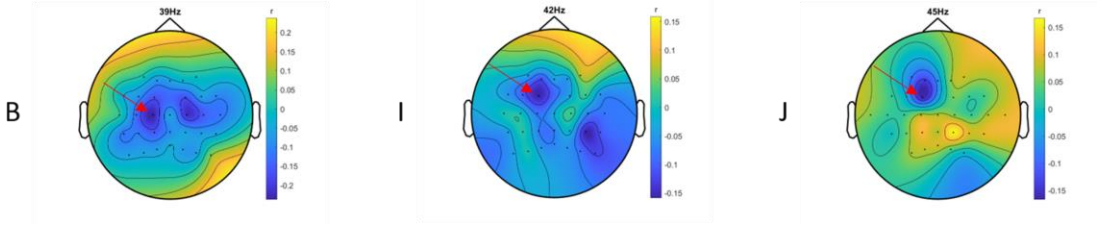

Figure 3.10 Lower gamma ERD during Session 5 BCI feedback for subjects B, I, J.

We then sought to determine if lower pre-grip release SMR amplitude (ERD) led to shorter muscle relaxation latencies. As expected, we found that successful yellow release trials had lower pre-grip release SMR amplitude than successful blue release trials ($p<0.025$, Fig. 3.11). In comparing the FDI relaxation latency for the blue circle versus the yellow circle condition, we found that grip release latency was not significantly shorter in the yellow circle

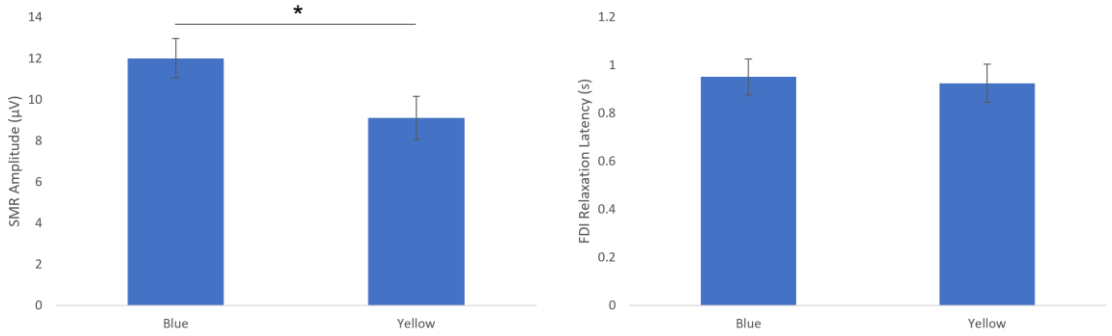

Figure 3.11 Sensorimotor rhythm amplitude and FDI relaxation latency. Left: Sensorimotor rhythm amplitude for blue (Clear Mind) vs. yellow (Imagine Release) targets. Right: FDI relaxation latency for blue vs. yellow targets. * indicates significant difference at $p<0.025$.

condition (p=0.124, **Fig. 3.11**), although creation of ERD tended to lead to a shorter relaxation time than generation of ERS (Δlatency = 0.026 ±0.046 seconds – mean± standard deviation)

We then tested whether the BCI training improved grip relaxation or performance on the BBT by comparing scores between Sessions 1 and 5. While we did not find a significant improvement in grip relaxation latency following BCI training (p=0.446, **Fig. 3.12**, left), average latency was reduced by roughly 10% in Session 5 as compared to Session 1 (Δlatency = 0.11±0.40 seconds). We did observe a significant improvement in BBT scores (p<0.05, **Fig. 3.12**, right). Participants improved their BBT by an average of 10 blocks, or 17%.

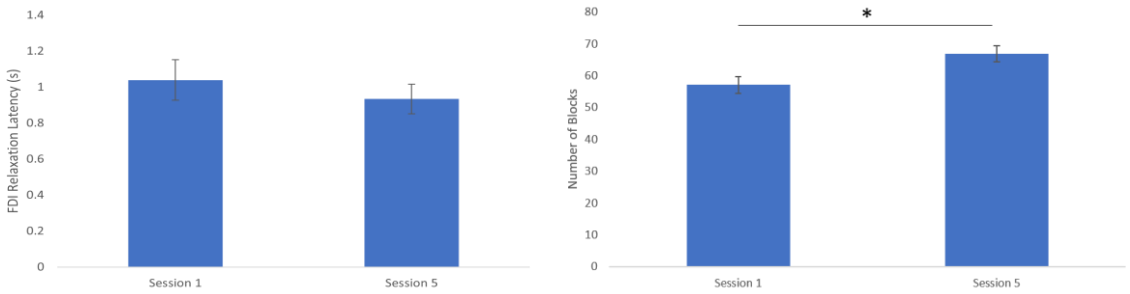

Figure 3.12 Session 1 and 5 FDI relaxation latency and Box-and-Blocks Test. (Left) FDI relaxation latency was not significantly different but showed a trend for improvement after BCI training. (Right) Box-and-Blocks Test was significantly improved following BCI training. * indicates significant difference at p<0.05.

3.3 Discussion

We were successfully able to demonstrate for the first time, to our knowledge, that subjects could use mental imagery during the planning period of grip release in order to control a BCI. The BCI control performance improved over the course of three training sessions. In a recent study that trained neurologically intact participants to control SMR amplitude preceding hand movement initiation, McFarland et al. found that participants were able to control the BCI with an accuracy 74.5% by the final evaluation session [58]. While we found a lower average BCI accuracy (58.4%) in the present study involving grip relaxation, it should be noted that their study involved 5-10 BCI training sessions and 4 evaluation sessions while our study had only 3

BCI training sessions and 1 evaluation session. Careful inspection of the correlation scalp topographies and spectra (**Fig. 3.9**) revealed that the electrodes and frequencies most predictive of task condition had shifted between Session 1 and Session 5. This therefore suggests that adaptation of the BCI control features should be performed in future studies.

In three of the four subjects who did not gain BCI control significantly above chance level, we found sharp correlation peaks localized to channel FC1 and C1 in the lower gamma frequency band. The appearance of low gamma range ERD slightly preceding and during muscle relaxation was noted previously in a study of young, healthy individuals [63]. Given that gamma correlation peaks only appeared in subjects with poor BCI accuracy, they may reflect a higher degree of effort or attention [67] during BCI control in these subjects.

It is interesting to note that Labyte *et al.* found beta ERD to occur significantly earlier in healthy elderly individuals with normal muscle relaxation compared to healthy young individuals [36], perhaps reflecting an increased need for planning in old age as a compensatory motor strategy. In comparison to Labyte *et al.*'s study, investigators examining older individuals with Parkinson's disease found that beta ERD was delayed on the more affected side relative to healthy individuals [24]. Thus, BCI training could be beneficial for earlier ERD creation to improve relaxation. While we did not observe a statistically significant relationship between SMR down-regulation and up-regulation and grip relaxation, there was a trend for reduced relaxation time with SMR down-regulation. Mean grip relaxation time also decreased from Session 1 to Session 5, although this difference was not significant. The effects of training may be more apparent in a patient population such as individuals with Parkinson's disease or stroke survivors. Indeed, McFarland and colleagues reported greatest improvement in movement initiation with BCI training for individuals with poorer initial performance [58]. Interestingly, we

did see significant improvement in hand task performance, as evidenced on the BBT, after training despite the participants performing only motor imagery or isometric grip force production. As the participant only performed the BBT during Session 1 and Session 5, which were generally separated by 2 weeks, it is unlikely the improvement arose from familiarity with the test.

Variability in the results may have arisen in part due to heterogeneity of the subject population. While subject ages were quite similar, we did not screen for factors known to influence the EEG signal, such as ADHD, caffeine use, drowsiness, or recent exercise. Additionally, the timing of the cue for grip release included some variability due to BCI2000 jitter [68]. In addition, participants had to respond to a visual cue rather than an auditory cue which is known to effect simple reaction time [69]. Indeed, our relaxation times were longer than those reported for a purely audio cue [17].

Despite these limitations, we did show that overall participants were able to modulate their SMR while maintaining an isometric grip force in preparation for release. BBT scores were significantly improved after BCI training. Therefore, we believe that this training protocol merits further study in rehabilitation for individuals experiencing delayed muscle relaxation such as Parkinson's disease patients and stroke survivors.

CHAPTER 4: EXAMINING THE EFFECTS OF GRIP RELAXATION BCI TRAINING USING CORTICOMUSCULAR COHERENCE

Abstract— The interaction between EEG and EMG signals conveys information about neural processing. We examined corticomuscular coherence (CMC) between selected EEG and EMG signals in neurotypical subjects performing grip force tasks, either maintaining an isometric grip force or tracking a dynamic force pattern. In comparing the static task to the dynamic task, we that CMC was significantly higher during the dynamic task in the gamma 2 band (49-65Hz) and in the FDI muscle. We also found that CMC was significantly lower in the beta band (14-31Hz) relative to the gamma 1 band (31-49Hz) across both the static and dynamic tasks. We then examined the effects of grip relaxation BCI training by comparing the dynamic task pre and post training. Although we saw significantly improved dynamic tracking performance, this did not correspond to significant CMC changes within the gamma 2 band. Finally, we examined the BCI feedback task directly within the beta band, which corresponded to the BCI control frequency. We found that trained event-related desynchronization (ERD) using grip release imagery and BCI feedback led to lower CMC compared to trained event-related synchronization (ERS). This finding elucidates potential mechanisms for performance improvements following BCI training and further motivates its extension to stroke survivors and Parkinson's patients.

4.1 Introduction

Corticomuscular coherence (CMC) describes the amount of supraspinal contributions to the output generated by spinal motor neurons [37]. The strength of CMC can vary between muscles [70-74], tasks [75-81], and trained and untrained individuals [74,82-83]. The anatomical basis for the differences between muscles includes differences in the density of corticospinal projections [84] and the density of muscle spindles [85]. Additionally, daily use of muscles in particular types of tasks can influence neural control strategies in a way that alters CMC. For example,

CMC of the dominant hand was found to be lower than that of the non-dominant hand of untrained individuals. CMC is greater in skilled weightlifters and lower in skilled musicians. [82].

Different tasks may preferentially evoke CMC in certain frequency bands [86]. CMC in the beta band (13-30Hz) is found during weak to moderate constant-force contractions. It is believed that beta band CMC supports an immutable, stable output from the motor cortex that requires minimal computational effort. In contrast, CMC in the gamma band (31-70Hz), also known as the Piper rhythm, becomes more evident during strong isometric contractions [67,87], slow phasic movement [87], isometric dynamic force production [88-91], and periods of readiness prior to increasing muscle activation in response to a stimulus [92]. It is believed that gamma CMC may support motor outputs that require binding together of spatially distributed cortical elements in order to perform tasks whose inputs and outputs change on a moment-by-moment basis, thereby requiring higher levels of attention [86].

We explored CMC generation in different muscles across different grip tasks. These tasks included maintenance of a static grip force and dynamic tracking of a specified grip pattern. We hypothesized that the dynamic task would result in greater CMC at high frequencies compared to the static task. We also hypothesized that subjects would have lower CMC after training due to improved motor control. Additionally, subjects performed a set of trials in which they used motor imagery to manipulate EEG signals prior to initiating release of grip force. We hypothesized that grip release imagery would reduce the CMC relative to a cleared mind mental state.

4.2 Methods

4.2.1 Participants

As part of a BCI-training study, n=10 neurotypical young adults participated in experimental sessions in which they attempted to control EEG signals while performing grip force tasks. Participants were right-handed and at least 18 years old, with no history of neurological disease, orthopedic impairment or pain of the hand preventing movement, or visual impairment. All participants provided their written informed consent. This study was approved by the Institutional Review Board of North Carolina State University.

We performed CMC analysis using the EEG and EMG data collected from n=9 subjects. We excluded one subject from our analysis due to technical difficulties collecting his EMG signals. The dataset was comprised of 32 EEG channels covering bilateral sensorimotor areas, 3 bipolar EMG channels targeting extensor digitorum communis (EDC), flexor digitorum superficialis (FDS), and first dorsal interosseous (FDI), and grip force recordings.

4.2.2 Static and Dynamic Tasks

The static task (**Fig. 4.1**, top) was performed in the first session of the BCI study and served as one-half of the trials used to calibrate the BCI. To briefly summarize, participants were required to hold a circle whose vertical height corresponds to grip force inside of a force target box of 20% +/- 3% of their maximum grip force. If subjects moved outside of the box during the keep gripping period, then the trial was aborted and discarded. Participants performed nine runs of 20 trials, approximately half of which were used for the static task. Participants rested for approximately 1-2 minute between runs to prevent fatigue. From each trial, we analyzed the 4-second period comprising the keep gripping warning and imperative periods.

The dynamic task (**Fig. 4.1**, bottom) was performed at the beginning of the first session and the fifth (final) session of the foregoing BCI study. To begin each trial, participants were required to increase their grip force in order to hold a force indicator circle inside of a force target box centered at 15% +/- 2% of their maximum grip force for 2 seconds. The circle then turned yellow and the target box began to oscillate sinusoidally with a peak-to-peak amplitude of 10% maximum grip force and a frequency of 0.5Hz for 15 seconds. Participants were instructed to modulate their grip force to maintain the circle in the center of the box as best as possible. Trials were not aborted if participants moved outside of the target box as it was moving. Subjects performed one run of 5 trials and one run of 10 trials, separated by a 1-2 rest break, for both sessions 1 and 5. We analyzed the 15-second period that participants were modulating their grip force in order to track the moving target.

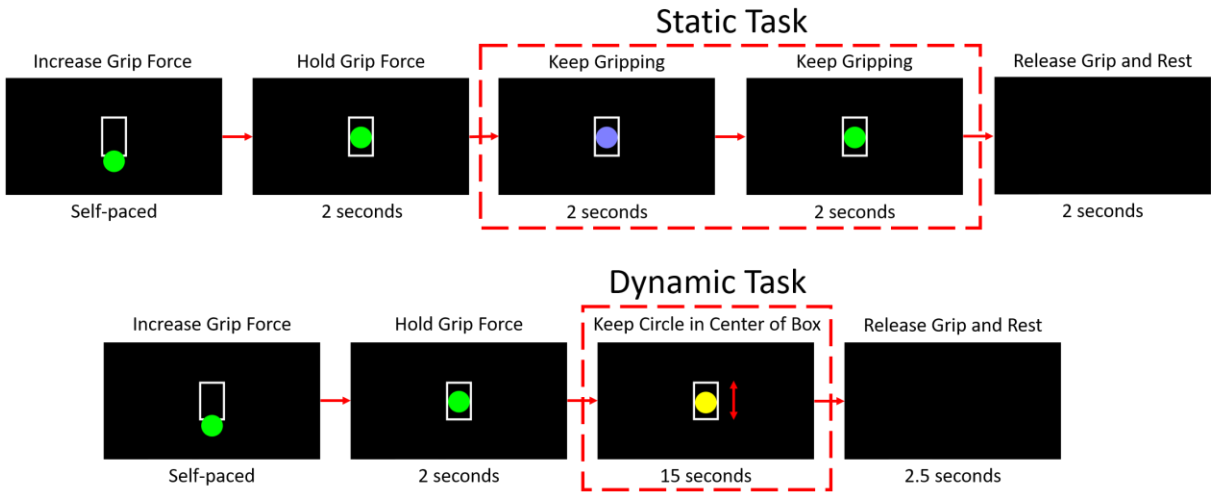

Figure 4.1 Static and dynamic tasks. Static task was 20% max grip force. Dynamic task was 15% +/- 5% max grip force with 0.5Hz frequency.

4.2.3 BCI Feedback Tasks

The BCI feedback tasks analyzed in this study were recorded during session 5 of the previous study (**Fig. 4.2**). Participants were asked to increase their grip force to 20% +/- 3% of their maximum and hold it there for 1 second. They were then shown a dim blue or a dim yellow circle and instructed to clear their mind (blue) or imagine releasing the grip (yellow) in order to brighten the circle which was controlled by their sensorimotor rhythm (SMR) amplitude. Participants performed 9 runs of 20 trials with 1-2 minute rest breaks between runs. We further analyzed the final 2 seconds of the BCI control period of both blue and yellow circle trials regardless of trial outcome. Trials that were aborted due to subject moving outside of the force target box prematurely were discarded.

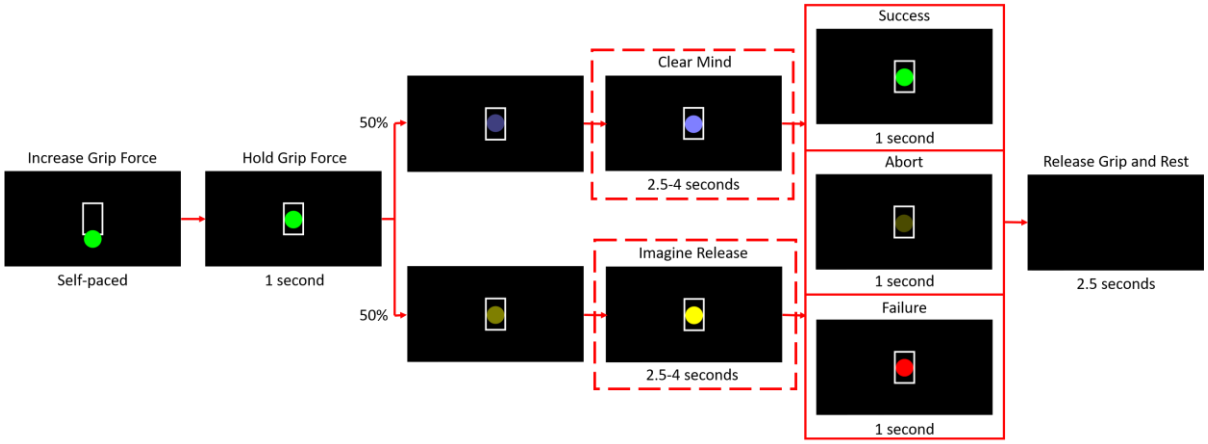

Figure 4.2 Clear mind and grip release motor imagery tasks. The final 2 seconds of the dashed boxes were used for CMC analysis.

4.2.4 EEG Pre-Processing

EEG and EMG signals were first combined into a single dataset and imported into the MATLAB toolbox EEGLAB [80] for Sessions 1 and 5 separately. The EEG signal pre-processing pipeline consisted of the following steps: 1) high-pass filtering at 1Hz; 2) interpolation of EEG channels that had poor contact with the scalp; 3) removing bad sections of

data containing bursts and artifacts affecting greater than 25% of the EEG channels using the EEGLAB plugin *Clean Rawdata*; 4) re-referencing the EEG signals to the common average and adding back in the recording reference electrode FCz; 5) removing 60Hz line noise with the EEGLAB plugin *Cleanline*; 6) performing principle component analysis to reduce the dimensionality of the data based on the number of interpolated electrodes and decomposing the resulting dataset using independent component analysis with the infomax algorithm implemented in EEGLAB as *runica*; 7) manual inspection of component activations, scalp maps, and spectra to identify and remove artifactual components; 8) extractions of epochs of interest; 9) semi-automated epoch rejection based on remaining independent components to remove any residual artifactual activity; 10) re-referencing the data using a small Laplacian spatial filter based on the Hjorth approximation. The resulting dataset contained 33 EEG channels of artifact-free epochs with the accompanying 3 channels of EMG.

4.2.5 Coherence

We computed the coherence spectrum as the magnitude of coherency for each subject, each task, and each pair of EEG and EMG signals using the following formula:

$$\left|\hat{R}_{XY}(f)\right| = \frac{\left|\hat{S}_{XY}(f)\right|}{\sqrt{\hat{S}_{XX}(f)\,\hat{S}_{YY}(f)}}$$

where $|\hat{S}_{XY}(f)|$ is the magnitude of the cross-spectral density between signals X and Y, $\hat{S}_{XX}(f)$ is the auto-spectral density of signal X and $\hat{S}_{YY}(f)$ is the auto-spectral density of signal Y. This was implemented using Bartlett's method of periodogram averaging of non-overlapped segments of 0.4s in duration. This yielded a frequency resolution of 2.5Hz. A 0.4s window was chosen as a trade-off of frequency resolution and capturing transient bursts of gamma activity which might otherwise be attenuated in a longer window. For this study, we did not implement a more advanced spectral estimation method, such as the multitaper method, which requires a window

length and a spectral smoothing parameter, both of which can differentially affect the magnitude of coherence based on the frequency making direct comparisons between frequency bands more difficult to interpret. We averaged coherence frequency bins within three frequency bands: beta (14-31Hz), gamma 1 (31-49Hz), and gamma 2 (49-65Hz). The 60Hz bin was not included in the average within the gamma 2 band to exclude potential line noise contamination of the signals.

4.2.6 Statistics

We first compared CMC during the static task to that during the dynamic task, both performed during Session 5. In order to simplify the analysis, we identified a single EEG electrode that displayed maximal coherence when taking an overall average across all muscles, frequency bands, tasks, and subjects. Our analysis considered average coherence between this EEG channel and the three EMG channels across three frequency bands: beta (14-31Hz), gamma 1 (31-49Hz), and gamma 2 (49-65Hz). We ran a repeated measures ANOVA (rmANOVA) with three within-subject factors: Task (static/ dynamic), Frequency (beta/ gamma / gamma 2), and Muscle (EDC/ FDS/ FDI).

To evaluate if there were changes in EEG-EMG coherence following BCI training, we compared the coherence during the dynamic task of Session 1 to coherence during the dynamic task of Session 5. We focused our analysis in the gamma 2 band because of the large coherence increase that we observed in gamma 2 when comparing the static task to the dynamic task. We again identified a single EEG electrode displaying maximal coherence by taking an overall average across muscles, sessions, and subjects within the gamma 2 band. We then ran an rmANOVA on the EEG-EMG coherence from the selected electrode using two within-subject factors: Session (Session 1/ Session 5) and Muscle (EDC/ FDS/ FDI). To determine if potential changes in coherence corresponded to task performance, we computed root-mean squared error

(RMSE) between the desired and the actual force profiles and performed a paired t-test on RMSE for Session 1 vs. Session 5.

For the BCI feedback data of Session 5, we chose to focus on the beta frequency band because this was the frequency band used in all subjects during BCI training. Again, we identified one electrode location displaying maximal coherence by taking an overall average across muscles, target conditions, and subjects. We then conducted a two-way rmANOVA with the within-subject factors: Condition (Blue/ Yellow) and Muscle (EDC/ FDS/ FDI).

For all ANOVAs, approximate multivariate variate normality was confirmed using histograms. Mauchley's test was used to confirm sphericity. Greenhouse-Geisser correction was used in instances where the sphericity assumption was violated. For all significant effects, pairwise comparisons were performed with Bonferroni correction.

4.3 Results

We identified channel C1 as having the highest overall coherence for the static and dynamic tasks of Session 1 (**Fig. 4.3**). In performing ANOVA, we found a significant Task x Frequency interaction. Pairwise comparisons revealed a significantly higher coherence during the dynamic task relative to the static task in the gamma 2 band. Additionally, we found a significant Task x Muscle interaction. We found that the FDI muscle had a significantly higher coherence during the dynamic task compared to the static task. We also found a significant main effect of frequency. Pairwise comparisons revealed that the gamma 1 band had significantly higher coherence than the beta band when averaged across tasks and muscles (**Fig. 4.4**).

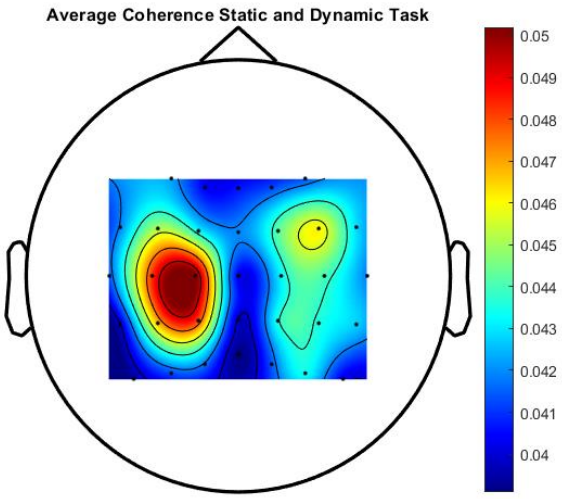

Fig. 4.3 Average Static Task and Dynamic Task CMC scalp map from Session 1. CMC was averaged across muscles, frequencies, tasks, and subjects.

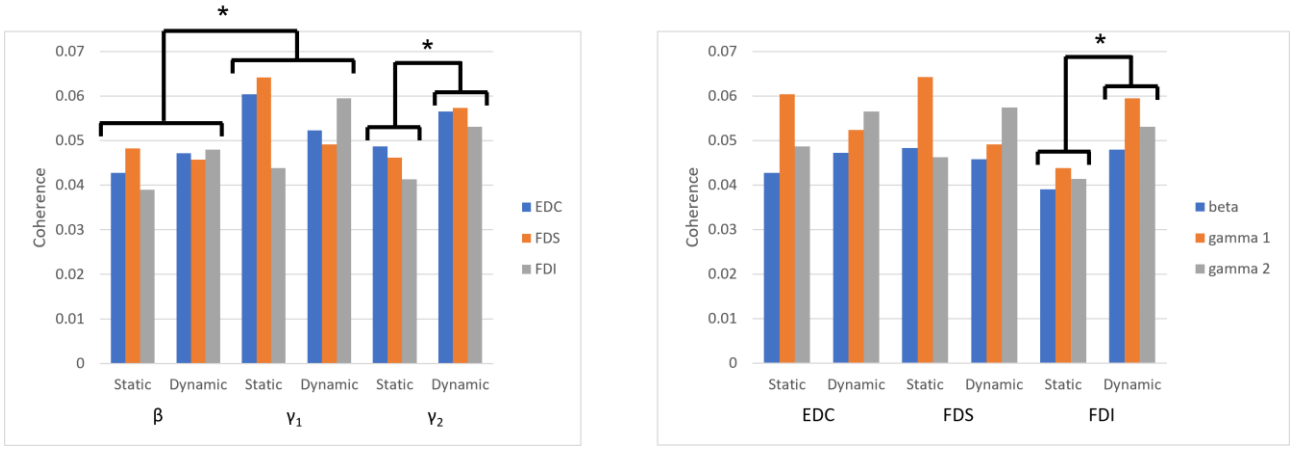

Fig. 4.4 Static vs. dynamic tasks peak CMC comparison. Data is from Session 1. * indicates significant difference at $p<0.05$.

In analyzing the gamma 2 band during the dynamic task of Sessions 1 and 5, we again identified channel C1 as displaying the peak coherence (**Fig. 4.5**). The two-factor rmANOVA did not show a significant effect of either Session or Muscle on coherence. However, there was a trend for lower coherence during Session 5 across all muscles, especially FDS and FDI (**Fig.**

4.6). The paired t-test revealed a significantly lower RMSE for dynamic force tracking in Session 5 (**Fig. 4.6**).

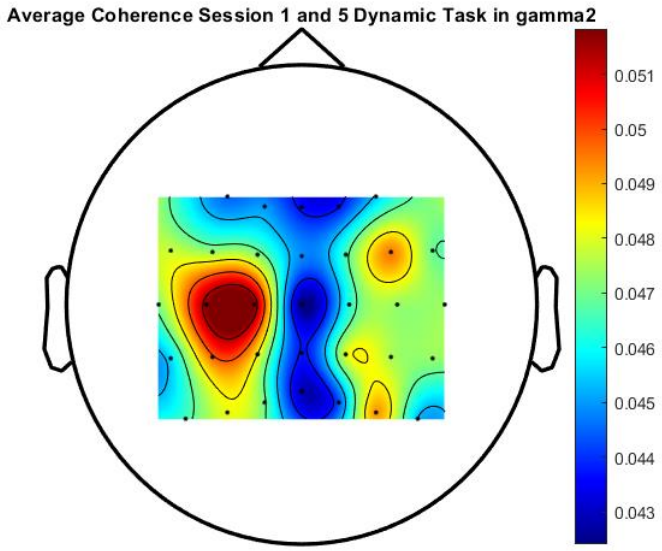

Figure 4.5 Average Session 1 and Session 5 CMC scalp map from Dynamic Task. CMC was averaged across muscles, frequencies, sessions, and subjects.

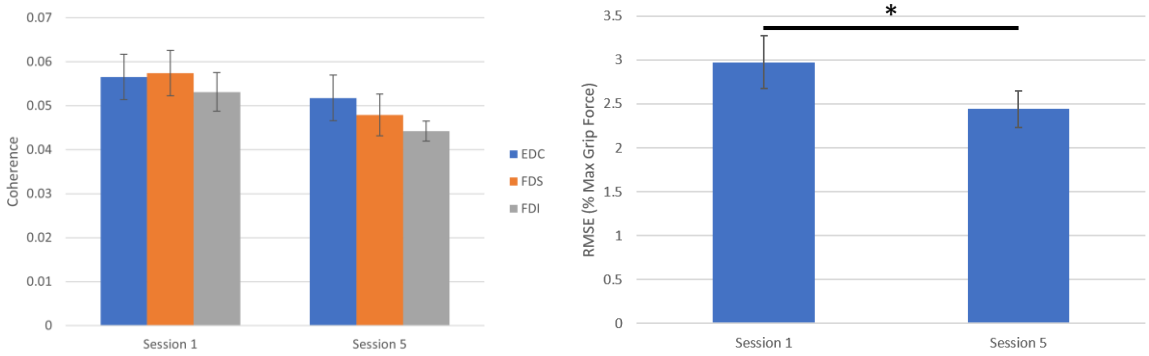

Fig. 4.6 Pre vs. Post-BCI training gamma 2 CMC and dynamic tracking performance. (Left) Gamma 2 CMC for EDC, FDS, and FDI muscle. (Right) Dynamic task RMSE as a percentage of maximum grip force pre vs. post-BCI training. Post-BCI training had significantly lower RMSE. * indicates significant difference at $p<0.05$.

We found that channel FC1 displayed the highest overall average coherence across the trials examining modulation of sensorimotor rhythms (**Fig. 4.7**). We found a significant main effect of Condition ($p<0.05$) with the beta band CMC value being significantly lower for the yellow circle condition (mental imagery of release). This impact was most readily observed for the EEG-EMG coherence involving FDS and EDC (Fig. 4.8). Neither Muscle nor the Condition x Muscle interaction significantly impacted coherence during these trials.

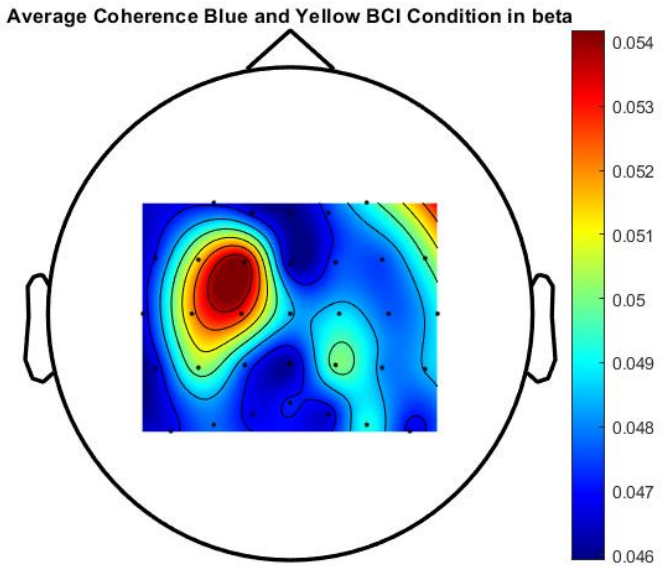

Fig. 4.7 BCI feedback task beta band (14-31Hz) CMC scalp maps for blue (clear mind) vs. yellow (imagine release) conditions.

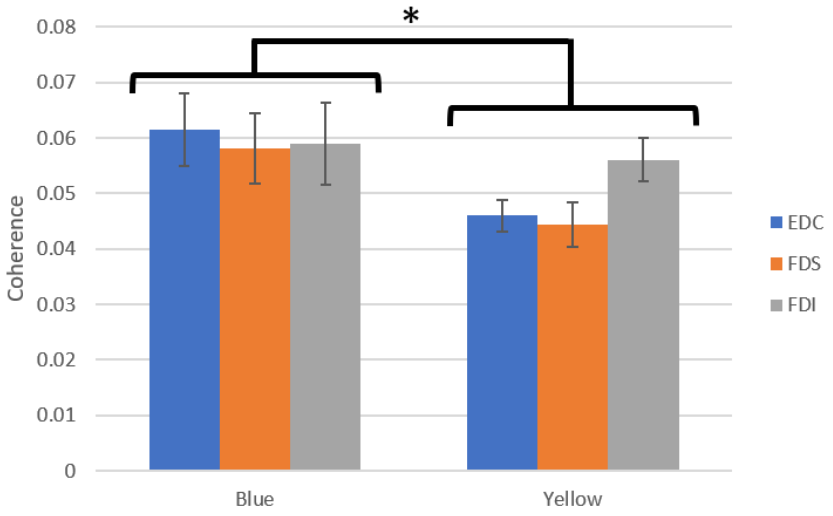

Fig. 4.8 Peak beta band CMC comparison for blue vs. yellow conditions during BCI feedback for EDC, FDS, and FDI. * indicates significant difference at $p<0.05$.

4.4 Discussion

We found that CMC within the gamma 2 band was significantly higher during the dynamic task compared to the static task. This finding accords with past studies of CMC during dynamic postural perturbations of the finger [88-91], although investigators in those studies largely focused on the gamma 1 rather than the gamma 2 range. It is possible that our dynamic task required higher levels of effort and attention, thereby resulting in CMC increases occurring at higher frequencies [86]. We also found an overall higher level of CMC in the gamma 1 band compared to the beta band. The gamma-range CMC in the dynamic task was expected [88-91], but higher gamma 1 CMC than beta CMC during the static task was unexpected. Our static task was recorded during the BCI calibration runs, in which there was a 50% likelihood that trials would require an immediate grip relaxation. It is possible that the structure of the task could have increased participants' readiness to respond, thereby evoking higher levels of gamma CMC [92]. Alternatively, it is possible that methodological differences in EMG signal recording could

explain the discrepancy. Most other studies use a lower cut-off frequency of 5Hz or lower when investigating beta band CMC. We used a higher (20Hz) cut-off frequency to reduce motion artifact, as have other studies, sometimes going up to 30 Hz for the cut-off frequency [73,76,93]. The different filter settings make comparisons difficult.

We additionally found that the FDI muscle had a higher level of coherence during the dynamic task than during the static task. It is possible that subjects were relying on modulation of FDI more than FDS or EDC in order to perform the dynamic task, but further studies are needed to confirm this.

The BCI training sessions did not lead to any significant changes in CMC for the dynamic trials, at least within the gamma 2 band. We did, however, observe a trend for lower CMC during Session 5. This reduction coincided with a significant improvement in dynamic force tracking performance, which occurred despite not practicing dynamic force tracking. The literature is mixed regarding whether CMC increases or decreases with motor skill learning. Perez *et al.* found that CMC increased within a single training session after visuomotor skill learning [83]. However, Semmler [82] and Ushiyama [7] found that trained individuals had significantly lower CMC relative to untrained individuals. It is possible that generalized improvements in grip force control as a result of BCI training could have carried over into improving dynamic grip force control. Better grip force control would generally result in lower CMC in the gamma 2 band.

We found that trained SMR down-regulation using motor imagery of grip release and visual feedback decreased CMC relative to SMR up-regulation. It is possible that SMR down-regulation reduced common drive to the motor neurons innervating the recorded muscles by activating intracortical inhibitory neurons [25,27]. However, it has been proposed that activation

of cortical inhibitory interneurons may not produce a measurable EEG signal due to the orientation of the dendrites of inhibitory interneurons being more variable than those of pyramidal cells [22]. Another possibility is that SMR down-regulation caused an increased activation of spinal inhibitory inter-neurons thereby reducing common drive to muscles [26,28,29]. In future studies, we will utilize transcranial stimulation or the H-reflex method to further explore the mechanism by which SMR down-regulation reduced the CMC.

For these analyses, we chose to focus on a single EEG channel for assessing EEG-EMG coherence. The channel was selected according to the peak coherence observed across subjects and conditions for a given set of trials. The same EEG channel was then used for all subjects. For comparing static and dynamic tasks and examining the impact of BCI training, we used channel C1. For the SMR modulation trials, we used channel FC1. These channels are likely involved in CMC based on their nominal anatomical position overlying contralateral primary motor cortex and contralateral premotor dorsal/supplementary motor area, respectively [65]. Future studies may address other EEG electrodes, including ipsilateral channels which may be important for stroke.

CHAPTER 5: CONCLUSION

In this work we have outlined the design and development of several novel tools targeting aberrant neural activation and deactivation patterns observed in a variety of neurological disorders. In chapter 2, we described a system for training proper EEG and EMG activation pattens that used a hand exoskeleton to provide movement assistance and afferent feedback to support Hebbian neuroplasticity. We then conducted an evaluation study of the system with neurotypical individuals. The subjects demonstrated that they could use the system and improved device control over the course of a single session. In chapter 3, we developed a novel BCI application that trains users to modulate cortical activation patterns during an isometric hold by imagining grip release. We were able to show that subjects could learn the task and improved with training. Furthermore, we showed that the intervention significantly improved upper extremity dexterity as measured by the box-and-blocks test. Finally, in Chapter 4 we investigated potential mechanisms for the hand dexterity improvements observed in Chapter 3 using corticomuscular coherence (CMC). We found that participants performed a dynamic grip force visuomotor tracking task with significantly less tracking error following BCI training of grip relaxation. There was a corresponding trend for lower CMC in the gamma 2 frequency band. Furthermore, we showed that beta band CMC was significantly lower during the motor imagery BCI condition relative to the clear mind condition. This demonstrates that CMC was being modulated during BCI training in addition to the directly targeted spectral amplitude.

For future work, we will conduct a multi-session study using the system presented in Chapter 2 in stroke survivors and evaluate for therapeutic benefit. We plan to improve our hand exoskeleton by using a custom 3D printed hybrid hand exoskeleton [94]. Furthermore, we plan to incorporate the novel BCI training task that was presented in Chapter 3 into the protocol. BCI

classification accuracy for all tasks will be improved in future studies by adapting the control features if necessary. Although we were able to show improved performance in neurotypical subjects, we believe that combined BCI and EMG feedback training will yield even greater benefits in stroke survivors.

REFERENCES

[1] Tsao CW, et al., Heart Disease and Stroke Statistics—2023 Update: A Report From the American Heart Association. Circulation. 2023;147: e93-e621. doi: 10.1161/CIR. 0000000000001123

[2] National Institute of Child Health and Human Development. (2022). *Stroke*. Retrieved June, 28, 2023 from https://www.nichd.nih.gov/health/topics/stroke/conditioninfo/risk

[3] Kelly-Hayes M, Beiser A, Kase CS, Scaramucci A, D'Agostino RB, Wolf PA. The influence of gender and age on disability following ischemic stroke: the Framingham study. J Stroke Cerebrovasc Dis. 2003 May-Jun;12(3):119-26. doi: 10.1016/S1052-3057(03)00042-9. PMID: 17903915.

[4] Jackson G, Chari K. National Hospital Care Survey Demonstration Projects: Stroke Inpatient Hospitalizations. Natl Health Stat Report. 2019 Nov;(132):1-11. PMID: 32510306.

[5] Lai SM, et al., Persisting Consequences of Stroke Measured by the Stroke Impact Scale. Stroke, 2002; 33(7): 1840-1844.

[6] Dobkin BH, Clincal practice. Rehabilitation after stroke. N Engl J Med, 2005; 352(16): 1677-1684.

[7] Cruz EG, et al., Kinetic and kinematic workspaces of the index finger following stroke. Brain, 2005; 128(Pt 5): 1112-21.

[8] Seo NJ, Enders LR, Motawar B, Kosmopoulos ML, Fathi-Firoozabad M. The extent of altered digit force direction correlates with clinical upper extremity impairment in chronic stroke survivors. J Biomech. 2015 Jan 21;48(2):383-7. doi: 10.1016/j.jbiomech.2014.11.046. Epub 2014 Dec 9. PMID: 25527892; PMCID: PMC4286432.

[9] Dewald JP, Pope PS, Given JD, Buchanan TS, Rymer WZ. Abnormal muscle coactivation patterns during isometric torque generation at the elbow and shoulder in hemiparetic subjects. Brain. 1995 Apr;118 (Pt 2):495-510. doi: 10.1093/brain/118.2.495. PMID: 7735890.

[10] Chae, J., Yang, G., Park, B.K. and Labatia, I. (2002), Delay in initiation and termination of muscle contraction, motor impairment, and physical disability in upper limb hemiparesis. Muscle Nerve, 25: 568-575. https://doi-org.prox.lib.ncsu.edu/10.1002/mus.10061

[11] Pfurtscheller G, Sager W, Wege W. Correlations between CT scan and sensorimotor EEG rhythms in patients with cerebrovascular disorders. Electroencephalogr Clin Neurophysiol. 1981 Nov;52(5):473-85. doi: 10.1016/0013-4694(81)90032-8. PMID: 6171414.

[12] Scherer, R., Mohapp, A., Grieshofer, P., Pfurtscheller, G., & Neuper, C. Sensorimotor EEG patterns during motor imagery in hemiparetic stroke patients. International Journal of Bioelectromagnetism. 2007; 9(3): 155-162.

[13] Kaiser V, Daly I, Pichiorri F, Mattia D, Müller-Putz GR, Neuper C. Relationship between electrical brain responses to motor imagery and motor impairment in stroke. Stroke. 2012 Oct;43(10):2735-40. doi: 10.1161/STROKEAHA.112.665489. Epub 2012 Aug 14. PMID: 22895995.

[14] Kamper DG, et al., Relative contributions of neural mechanisms versus muscle mechanics in promoting finger extension deficits following stroke. Muscle Nerve, 2003; 28(3): 309-18.

[15] Kamper DG and Rymer WZ, Impairment of voluntary control of finger motion following stroke: Role of inappropriate muscle coactivation. Muscle Nerve, 2001; 24(5): 673-81.

[16] Hoffman G, et al., Contributions of voluntary activation deficits to hand weakness after stroke. Topics in Stroke Rehabil, 2016; 23(6): 384-392.

[17] Seo NJ, Rymer WZ, Kamper DG. Delays in grip initiation and termination in persons with stroke: effects of arm support and active muscle stretch exercise. J Neurophysiol. 2009 Jun;101(6):3108-15. doi: 10.1152/jn.91108.2008. Epub 2009 Apr 8. PMID: 19357330.

[18] K. Terada, A. Ikeda, T. Nagamine, H. Shibasaki, Movement-related cortical potentials associated with voluntary muscle relaxation. Electroencephalography and Clinical Neurophysiology. Volume 95, Issue 5, 1995, Pages 335-345, https://doi.org/10.1016/0013-4694(95)00098-J.

[19] Yazawa S, Ikeda A, Kunieda T, Mima T, Nagamine T, Ohara S, Terada K, Taki W, Kimura J, Shibasaki H. Human supplementary motor area is active in preparation for both voluntary muscle relaxation and contraction: subdural recording of Bereitschaftspotential. Neurosci Lett. 1998 Mar 20;244(3):145-8. doi: 10.1016/s0304-3940(98)00149-9. PMID: 9593510.

[20] Rothwell JC, Higuchi K, Obeso JA. The offset cortical potential: an electrical correlate of movement inhibition in man. Mov Disord. 1998 Mar;13(2):330-5. doi: 10.1002/mds.870130221. PMID: 9539349.

[21] Toma K, Honda M, Hanakawa T, Okada T, Fukuyama H, Ikeda A, Nishizawa S, Konishi J, Shibasaki H. Activities of the primary and supplementary motor areas increase in preparation and execution of voluntary muscle relaxation: an event-related fMRI study. J Neurosci. 1999 May 1;19(9):3527-34. doi: 10.1523/JNEUROSCI.19-09-03527.1999. PMID: 10212312; PMCID: PMC6782247.

[22] Pope PA, Holton A, Hassan S, Kourtis D, Praamstra P. Cortical control of muscle relaxation: a lateralized readiness potential (LRP) investigation. Clin Neurophysiol. 2007 May;118(5):1044-52. doi: 10.1016/j.clinph.2007.02.002. Epub 2007 Mar 26. PMID: 17382586.

[23] Vogt T, Kato K, Flüthmann N, Bloch O, Nakata H, Kanosue K. Performance control in one consecutive motor task sequence - Approaching central neuronal motor behaviour preceding isometric contraction onsets and relaxation offsets at lower distinct torques. J Musculoskelet Neuronal Interact. 2018 Mar 1;18(1):1-8. PMID: 29504573; PMCID: PMC5881123.

[24] Labyt E, et al., Abnormal cortical mechanisms in voluntary muscle relaxation in de novo parkinsonian patients. J Clin Neurophysiol, 2005; 22(3): 192-203.

[25] Buccolieri A, Abbruzzese G, Rothwell JC. Relaxation from a voluntary contraction is preceded by increased excitability of motor cortical inhibitory circuits. J Physiol. 2004 Jul 15;558(Pt 2):685-95. doi: 10.1113/jphysiol.2004.064774. Epub 2004 Jun 4. PMID: 15181164; PMCID: PMC1664966.

[26] Begum T, Mima T, Oga T, Hara H, Satow T, Ikeda A, Nagamine T, Fukuyama H, Shibasaki H. Cortical mechanisms of unilateral voluntary motor inhibition in humans. Neurosci Res. 2005 Dec;53(4):428-35. doi: 10.1016/j.neures.2005.09.002. Epub 2005 Oct 4. PMID: 16213048.

[27] Motawar B, Hur P, Stinear J, Seo NJ. Contribution of intracortical inhibition in voluntary muscle relaxation. Exp Brain Res. 2012 Sep;221(3):299-308. doi: 10.1007/s00221-012-3173-x. Epub 2012 Jul 13. PMID: 22791231; PMCID: PMC8103219.

[28] Suzuki T, Sugawara K, Takagi M, Higashi T. Excitability changes in primary motor cortex just prior to voluntary muscle relaxation. J Neurophysiol. 2015 Jan 1;113(1):110-5. doi: 10.1152/jn.00489.2014. Epub 2014 Oct 8. PMID: 25298384.

[29] Suzuki T, Sugawara K, Ogahara K, Higashi T. Time Course of Corticospinal Excitability and Intracortical Inhibition Just before Muscle Relaxation. Front Hum Neurosci. 2016 Jan 28;10:1. doi: 10.3389/fnhum.2016.00001. PMID: 26858619; PMCID: PMC4729883.

[30] Schieppati M, Crenna P. From activity to rest: gating of excitatory autogenetic afferences from the relaxing muscle in man. Exp Brain Res. 1984;56(3):448-57. doi: 10.1007/BF00237985. PMID: 6499972.

[31] Schieppati M, Nardone A, Musazzi M. Modulation of the Hoffmann reflex by rapid muscle contraction or release. Hum Neurobiol. 1986;5(1):59-66. PMID: 3700149.

[32] Hummel FC, Steven B, Hoppe J, Heise K, Thomalla G, Cohen LG, Gerloff C. Deficient intracortical inhibition (SICI) during movement preparation after chronic stroke. Neurology. 2009 May 19;72(20):1766-72. doi: 10.1212/WNL.0b013e3181a609c5. PMID: 19451532; PMCID: PMC2683737.

[33] Seo NJ, Fischer HW, Bogey RA, Rymer WZ, Kamper DG. Effect of a serotonin antagonist on delay in grip muscle relaxation for persons with chronic hemiparetic stroke. Clin Neurophysiol. 2011 Apr;122(4):796-802. doi: 10.1016/j.clinph.2010.10.035. Epub 2010 Nov 13. PMID: 21075681.

[34] Lelli S, Panizza M, Hallett M. Spinal cord inhibitory mechanisms in Parkinson's disease. Neurology. 1991 Apr;41(4):553-6. doi: 10.1212/wnl.41.4.553. PMID: 2011256.

[35] Kleine BU, Praamstra P, Stegeman DF, Zwarts MJ. Impaired motor cortical inhibition in Parkinson's disease: motor unit responses to transcranial magnetic stimulation. Exp Brain Res. 2001 Jun;138(4):477-83. doi: 10.1007/s002210100731. PMID: 11465746.

[36] Labyt E, Cassim F, Szurhaj W, Bourriez JL, Derambure P. Oscillatory cortical activity related to voluntary muscle relaxation: influence of normal aging. Clin Neurophysiol. 2006 Sep;117(9):1922-30. doi: 10.1016/j.clinph.2006.05.017. Epub 2006 Aug 1. PMID: 16887382.

[37] Farina D, Merletti R, Enoka RM. The extraction of neural strategies from the surface EMG: an update. J Appl Physiol (1985). 2014 Dec 1;117(11):1215-30. doi:

10.1152/japplphysiol.00162.2014. Epub 2014 Oct 2. PMID: 25277737; PMCID: PMC4254845.

[38] Dimitrov GV, Arabadzhiev TI, Hogrel JY, Dimitrova NA. Simulation analysis of interference EMG during fatiguing voluntary contractions. Part II--changes in amplitude and spectral characteristics. J Electromyogr Kinesiol. 2008 Feb;18(1):35-43. doi: 10.1016/j.jelekin.2006.07.002. Epub 2006 Sep 11. PMID: 16963280.

[39] Farina D, Rainoldi A. Compensation of the effect of sub-cutaneous tissue layers on surface EMG: a simulation study. Med Eng Phys. 1999 Jul-Sep;21(6-7):487-97. doi: 10.1016/s1350-4533(99)00075-2. PMID: 10624744.

[40] Negro F, Farina D. Linear transmission of cortical oscillations to the neural drive to muscles is mediated by common projections to populations of motoneurons in humans. J Physiol. 2011 Feb 1;589(Pt 3):629-37. doi: 10.1113/jphysiol.2010.202473. Epub 2010 Dec 6. PMID: 21135042; PMCID: PMC3055547.

[41] Thielbar KO Benefits of Using a Voice and EMG-Driven Actuated Glove to Support Occupational Therapy for Stroke Survivors. IEEE Transaction on Neural Systems and Rehabilitation Engineering, 2017; 25(3): 297-305.

[42] Susanto EA, et al., Efficacy of robot-assisted fingers training in chronic stroke survivors: a pilot randomized-controlled trial. J NeuroEngineering Rehabil, 2015; 12(42).

[43] Norman SL, et al., Controlling pre-movement sensorimotor rhythm can improve finger extension after stroke. J Neural Eng, 2018; 15(5)

[44] Ramos-Murguialday A, Broetz D, Rea M, Läer L, Yilmaz O, Brasil FL, Liberati G, Curado MR, Garcia-Cossio E, Vyziotis A, Cho W, Agostini M, Soares E, Soekadar S, Caria A, Cohen LG, Birbaumer N. Brain-machine interface in chronic stroke rehabilitation: a

controlled study. Ann Neurol. 2013 Jul;74(1):100-8. doi: 10.1002/ana.23879. Epub 2013 Aug 7. PMID: 23494615; PMCID: PMC3700597.

[45] Ono T, Shindo K, Kawashima K, Ota N, Ito M, Ota T, Mukaino M, Fujiwara T, Kimura A, Liu M, Ushiba J. Brain-computer interface with somatosensory feedback improves functional recovery from severe hemiplegia due to chronic stroke. Front Neuroeng. 2014 Jul 7;7:19. doi: 10.3389/fneng.2014.00019. PMID: 25071543; PMCID: PMC4083225.

[46] Pichiorri F, Morone G, Petti M, Toppi J, Pisotta I, Molinari M, Paolucci S, Inghilleri M, Astolfi L, Cincotti F, Mattia D. Brain-computer interface boosts motor imagery practice during stroke recovery. Ann Neurol. 2015 May;77(5):851-65. doi: 10.1002/ana.24390. Epub 2015 Mar 27. PMID: 25712802.

[47] Ang KK, Chua KS, Phua KS, Wang C, Chin ZY, Kuah CW, Low W, Guan C. A Randomized Controlled Trial of EEG-Based Motor Imagery Brain-Computer Interface Robotic Rehabilitation for Stroke. Clin EEG Neurosci. 2015 Oct;46(4):310-20. doi: 10.1177/1550059414522229. Epub 2014 Apr 21. PMID: 24756025.

[48] Daly JJ, Cheng R, Rogers J, Litinas K, Hrovat K, Dohring M. Feasibility of a new application of noninvasive Brain Computer Interface (BCI): a case study of training for recovery of volitional motor control after stroke. J Neurol Phys Ther. 2009 Dec;33(4):203-11. doi: 10.1097/NPT.0b013e3181c1fc0b. PMID: 20208465.

[49] Bai Z, Fong KNK, Zhang JJ, Chan J, Ting KH. Immediate and long-term effects of BCI-based rehabilitation of the upper extremity after stroke: a systematic review and meta-analysis. J Neuroeng Rehabil. 2020 Apr 25;17(1):57. doi: 10.1186/s12984-020-00686-2. PMID: 32334608; PMCID: PMC7183617.

[50] Ethier C, Gallego JA, Miller LE. Brain-controlled neuromuscular stimulation to drive neural plasticity and functional recovery. Curr Opin Neurobiol. 2015 Aug;33:95-102. doi: 10.1016/j.conb.2015.03.007. Epub 2015 Mar 28. PMID: 25827275; PMCID: PMC4523462.

[51] Schalk G., et al., BCI2000: A General-Purpose Brain-Computer Interface (BCI) System. IEEE Transactions on Biomedical Engineering, 2004; 51(6): 1034-1043.

[52] Combrisson E, Jerbi K. Exceeding chance level by chance: The caveat of theoretical chance levels in brain signal classification and statistical assessment of decoding accuracy. J Neurosci Methods. 2015 Jul 30;250:126-36. doi: 10.1016/j.jneumeth.2015.01.010. Epub 2015 Jan 14. PMID: 25596422.

[53] Ang K and Guan C, Brain–Computer Interface for Neurorehabilitation of Upper Limb After Stroke, in Proceedings of the IEEE 2015 June; 103(6): 944-953. doi: 10.1109/JPROC.2015.2415800.

[54] Müller-Putz G, *et al*., Towards Noninvasive Hybrid Brain–Computer Interfaces: Framework, Practice, Clinical Application, and Beyond, in Proceedings of the IEEE 2015 June; 103(6): 926-943.doi: 10.1109/JPROC.2015.2411333.

[55] Sarasola-Sanz A, Irastorza-Landa N, Lopez-Larraz E, Bibian C, Helmhold F, Broetz D, Birbaumer N, Ramos-Murguialday A. A hybrid brain-machine interface based on EEG and EMG activity for the motor rehabilitation of stroke patients. IEEE Int Conf Rehabil Robot. 2017 Jul;2017:895-900. doi: 10.1109/ICORR.2017.8009362. PMID: 28813934.

[56] Bhagat NA, Yozbatiran N, Sullivan JL, Paranjape R, Losey C, Hernandez Z, Keser Z, Grossman R, Francisco GE, O'Malley MK, Contreras-Vidal JL. Neural activity modulations and motor recovery following brain-exoskeleton interface mediated stroke rehabilitation.

Neuroimage Clin. 2020;28:102502. doi: 10.1016/j.nicl.2020.102502. Epub 2020 Nov 19. PMID: 33395991; PMCID: PMC7749405.

[57] Ang KK, Guan C, Chua KS, Ang BT, Kuah CW, Wang C, Phua KS, Chin ZY, Zhang H. A large clinical study on the ability of stroke patients to use an EEG-based motor imagery brain-computer interface. Clin EEG Neurosci. 2011 Oct;42(4):253-8. doi: 10.1177/155005941104200411. PMID: 22208123.

[58] McFarland DJ, et al., Effects of training pre-movement sensorimotor rhythms on behavioral performance: A pilot study. J Neural Eng, 2015; 12(6)

[59] McFarland DJ, Sarnacki WA, Vaughan TM, Wolpaw JR. Brain-computer interface (BCI) operation: signal and noise during early training sessions. Clin Neurophysiol. 2005 Jan;116(1):56-62. doi: 10.1016/j.clinph.2004.07.004. PMID: 15589184.

[60] Bundy DT, Souders L, Baranyai K, Leonard L, Schalk G, Coker R, Moran DW, Huskey T, Leuthardt EC. Contralesional Brain-Computer Interface Control of a Powered Exoskeleton for Motor Recovery in Chronic Stroke Survivors. Stroke. 2017 Jul;48(7):1908-1915. doi: 10.1161/STROKEAHA.116.016304. Epub 2017 May 26. PMID: 28550098; PMCID: PMC5482564.

[61] Wing AM. A comparison of the rate of pinch grip force increases and decreases in parkinsonian bradykinesia. Neuropsychologia. 1988;26(3):479-82. doi: 10.1016/0028-3932(88)90100-5. PMID: 3374806.

[62] Toma K, Nagamine T, Yazawa S, Terada K, Ikeda A, Honda M, Oga T, Shibasaki H. Desynchronization and synchronization of central 20-Hz rhythms associated with voluntary muscle relaxation: a magnetoencephalographic study. Exp Brain Res. 2000 Oct;134(4):417-25. doi: 10.1007/s002210000483. PMID: 11081823.

[63] Alegre M, Labarga A, Gurtubay IG, Iriarte J, Malanda A, Artieda J. Movement-related changes in cortical oscillatory activity in ballistic, sustained and negative movements. Exp Brain Res. 2003 Jan;148(1):17-25. doi: 10.1007/s00221-002-1255-x. Epub 2002 Nov 9. PMID: 12478393.

[64] Mathiowetz V, Volland G, Kashman N, Weber K. Adult norms for the Box and Block Test of manual dexterity. Am J Occup Ther. 1985 Jun;39(6):386-91. doi: 10.5014/ajot.39.6.386. PMID: 3160243.

[65] Scrivener CL, Reader AT. Variability of EEG electrode positions and their underlying brain regions: visualizing gel artifacts from a simultaneous EEG-fMRI dataset. Brain Behav. 2022 Feb;12(2):e2476. doi: 10.1002/brb3.2476. Epub 2022 Jan 18. PMID: 35040596; PMCID: PMC8865144.

[66] McFarland DJ, Wolpaw JR. Sensorimotor rhythm-based brain-computer interface (BCI): model order selection for autoregressive spectral analysis. J Neural Eng. 2008 Jun;5(2):155-62. doi: 10.1088/1741-2560/5/2/006. Epub 2008 Apr 22. PMID: 18430974; PMCID: PMC2747265.

[67] Mima T, Simpkins N, Oluwatimilehin T, Hallett M. Force level modulates human cortical oscillatory activities. Neurosci Lett. 1999 Nov 12;275(2):77-80. doi: 10.1016/s0304-3940(99)00734-x. PMID: 10568503.

[68] Wilson, J. Adam, Christoph Guger, and Gerwin Schalk, 'BCI Hardware and Software', in Jonathan Wolpaw, and Elizabeth Winter Wolpaw (eds), *Brain–Computer Interfaces: Principles and Practice* (2012; online edn, Oxford Academic, 24 May 2012), https://doi.org/10.1093/acprof:oso/9780195388855.003.0009, accessed 13 July 2023.

[69] Jain A, Bansal R, Kumar A, Singh KD. A comparative study of visual and auditory reaction times on the basis of gender and physical activity levels of medical first year students. Int J Appl Basic Med Res. 2015 May-Aug;5(2):124-7. doi: 10.4103/2229-516X.157168. PMID: 26097821; PMCID: PMC4456887.

[70] Salenius S, Portin K, Kajola M, Salmelin R, Hari R. Cortical control of human motoneuron firing during isometric contraction. J Neurophysiol. 1997 Jun;77(6):3401-5. doi: 10.1152/jn.1997.77.6.3401. PMID: 9212286.

[71] Kilner JM, Baker SN, Salenius S, Hari R, Lemon RN. Human cortical muscle coherence is directly related to specific motor parameters. J Neurosci. 2000 Dec 1;20(23):8838-45. doi: 10.1523/JNEUROSCI.20-23-08838.2000. PMID: 11102492; PMCID: PMC6773054.

[72] Grosse P, Guerrini R, Parmeggiani L, Bonanni P, Pogosyan A, Brown P. Abnormal corticomuscular and intermuscular coupling in high-frequency rhythmic myoclonus. Brain. 2003 Feb;126(Pt 2):326-42. doi: 10.1093/brain/awg043. PMID: 12538401.

[73] Riddle CN, Baker SN. Manipulation of peripheral neural feedback loops alters human corticomuscular coherence. J Physiol. 2005 Jul 15;566(Pt 2):625-39. doi: 10.1113/jphysiol.2005.089607. Epub 2005 May 26. PMID: 15919711; PMCID: PMC1464768.

[74] Ushiyama J, Takahashi Y, Ushiba J. Muscle dependency of corticomuscular coherence in upper and lower limb muscles and training-related alterations in ballet dancers and weightlifters. J Appl Physiol (1985). 2010 Oct;109(4):1086-95. doi: 10.1152/japplphysiol.00869.2009. Epub 2010 Aug 5. PMID: 20689093.

[75] Kilner JM, Baker SN, Salenius S, Jousmäki V, Hari R, Lemon RN. Task-dependent modulation of 15-30 Hz coherence between rectified EMGs from human hand and forearm

muscles. J Physiol. 1999 Apr 15;516 (Pt 2)(Pt 2):559-70. doi: 10.1111/j.1469-7793.1999.0559v.x. PMID: 10087353; PMCID: PMC2269269.

[76] Riddle CN, Baker SN. Digit displacement, not object compliance, underlies task dependent modulations in human corticomuscular coherence. Neuroimage. 2006 Nov 1;33(2):618-27. doi: 10.1016/j.neuroimage.2006.07.027. Epub 2006 Sep 11. PMID: 16963283.

[77] McClelland VM, Cvetkovic Z, Mills KR. Modulation of corticomuscular coherence by peripheral stimuli. Exp Brain Res. 2012 Jun;219(2):275-92. doi: 10.1007/s00221-012-3087-7. Epub 2012 Apr 24. PMID: 22526947.

[78] Androulidakis AG, Doyle LM, Yarrow K, Litvak V, Gilbertson TP, Brown P. Anticipatory changes in beta synchrony in the human corticospinal system and associated improvements in task performance. Eur J Neurosci. 2007 Jun;25(12):3758-65. doi: 10.1111/j.1460-9568.2007.05620.x. PMID: 17610595.

[79] Kristeva-Feige R, Fritsch C, Timmer J, Lücking CH. Effects of attention and precision of exerted force on beta range EEG-EMG synchronization during a maintained motor contraction task. Clin Neurophysiol. 2002 Jan;113(1):124-31. doi: 10.1016/s1388-2457(01)00722-2. PMID: 11801434.

[80] Reyes A, Laine CM, Kutch JJ, Valero-Cuevas FJ. Beta Band Corticomuscular Drive Reflects Muscle Coordination Strategies. Front Comput Neurosci. 2017 Apr 4;11:17. doi: 10.3389/fncom.2017.00017. PMID: 28420975; PMCID: PMC5378725.

[81] Kilner JM, Salenius S, Baker SN, Jackson A, Hari R, Lemon RN. Task-dependent modulations of cortical oscillatory activity in human subjects during a bimanual precision grip task. Neuroimage. 2003 Jan;18(1):67-73. doi: 10.1006/nimg.2002.1322. PMID: 12507444.

[82] Semmler JG, Sale MV, Meyer FG, Nordstrom MA. Motor-unit coherence and its relation with synchrony are influenced by training. J Neurophysiol. 2004 Dec;92(6):3320-31. doi: 10.1152/jn.00316.2004. Epub 2004 Jul 21. PMID: 15269232.

[83] Perez MA, Lundbye-Jensen J, Nielsen JB. Changes in corticospinal drive to spinal motoneurones following visuo-motor skill learning in humans. J Physiol. 2006 Jun 15;573(Pt 3):843-55. doi: 10.1113/jphysiol.2006.105361. Epub 2006 Mar 31. PMID: 16581867; PMCID: PMC1779755.

[84] Palmer E, Ashby P. Corticospinal projections to upper limb motoneurones in humans. J Physiol. 1992 Mar;448:397-412. doi: 10.1113/jphysiol.1992.sp019048. PMID: 1593472; PMCID: PMC1176206.

[85] Peck D, Buxton DF, Nitz A. A comparison of spindle concentrations in large and small muscles acting in parallel combinations. J Morphol. 1984 Jun;180(3):243-52. doi: 10.1002/jmor.1051800307. PMID: 6235379.

[86] Brown P. Cortical drives to human muscle: the Piper and related rhythms. Prog Neurobiol. 2000 Jan;60(1):97-108. doi: 10.1016/s0301-0082(99)00029-5. PMID: 10622378.

[87] Brown P, Salenius S, Rothwell JC, Hari R. Cortical correlate of the Piper rhythm in humans. J Neurophysiol. 1998 Dec;80(6):2911-7. doi: 10.1152/jn.1998.80.6.2911. PMID: 9862895.

[88] Andrykiewicz A, Patino L, Naranjo JR, Witte M, Hepp-Reymond MC, Kristeva R. Corticomuscular synchronization with small and large dynamic force output. BMC Neurosci. 2007 Nov 27;8:101. doi: 10.1186/1471-2202-8-101. PMID: 18042289; PMCID: PMC2245954.

[89] Chakarov V, Naranjo JR, Schulte-Mönting J, Omlor W, Huethe F, Kristeva R. Beta-range EEG-EMG coherence with isometric compensation for increasing modulated low-level

forces. J Neurophysiol. 2009 Aug;102(2):1115-20. doi: 10.1152/jn.91095.2008. Epub 2009 May 20. PMID: 19458142.

[90] Naranjo JR, Wang X, Schulte-Mönting J, Huethe F, Maurer C, Hepp-Reymond MC, Kristeva R. Corticospinal interaction during isometric compensation for modulated forces with different frequencies. BMC Neurosci. 2010 Dec 31;11:157. doi: 10.1186/1471-2202-11-157. PMID: 21194447; PMCID: PMC3023786.

[91] Omlor W, Patino L, Hepp-Reymond MC, Kristeva R. Gamma-range corticomuscular coherence during dynamic force output. Neuroimage. 2007 Feb 1;34(3):1191-8. doi: 10.1016/j.neuroimage.2006.10.018. Epub 2006 Dec 19. PMID: 17182258.

[92] Schoffelen JM, Oostenveld R, Fries P. Neuronal coherence as a mechanism of effective corticospinal interaction. Science. 2005 Apr 1;308(5718):111-3. doi: 10.1126/science.1107027. PMID: 15802603.

[93] Witham CL, Riddle CN, Baker MR, Baker SN. Contributions of descending and ascending pathways to corticomuscular coherence in humans. J Physiol. 2011 Aug 1;589(Pt 15):3789-800. doi: 10.1113/jphysiol.2011.211045. Epub 2011 May 30. PMID: 21624970; PMCID: PMC3171886.

[94] Vertongen, Jens and Kamper, Derek. "Design of a 3D printed hybrid mechanical structure for a hand exoskeleton" Current Directions in Biomedical Engineering, vol. 6, no. 2, 2020, pp. 20202003. https://doi.org/10.1515/cdbme-2020-2003